

# 000 001 002 003 004 005 006 007 008 009 010 011 012 013 014 015 016 017 018 019 020 021 022 023 024 025 026 027 028 029 030 031 032 033 034 035 036 037 038 039 040 041 042 043 044 045 046 047 048 049 050 051 052 053 UNDERSTANDING THE ROLE OF TRAINING DATA IN TEST-TIME SCALING

Anonymous authors

Paper under double-blind review

## ABSTRACT

Test-time scaling improves the reasoning capabilities of large language models (LLMs) by allocating extra compute to generate longer Chains-of-Thoughts (CoTs). This enables models to tackle more complex problem by breaking them down into additional steps, backtracking, and correcting mistakes. Despite its strong performance—demonstrated by OpenAI’s o1 and DeepSeek R1, the conditions in the training data under which long CoTs emerge, and when such long CoTs improve the performance, remain unclear. In this paper, we study the performance of test-time scaling for transformers trained on an in-context weight prediction task for linear regression. Our analysis provides a theoretical explanation for several intriguing observations: First, at any fixed test error, increasing test-time compute allows us to reduce the number of in-context examples (context length) in training prompts. Second, if the skills required to solve a downstream task are not sufficiently present in the training data, increasing test-time compute can harm performance. Finally, we characterize task hardness via the smallest eigenvalue of its feature covariance matrix and show that training on a diverse, relevant, and hard set of tasks results in best performance for test-time scaling. We confirm our findings with experiments on large, nonlinear transformer architectures.

## 1 INTRODUCTION

Scaling test-time compute enhances inference in large language models (LLMs), by enabling reasoning with long chains-of-thought (CoTs). This allows models to generate more intermediate reasoning steps for complex problems, evaluate multiple options, and backtrack to find more accurate answers, all without changing the model’s parameters. There has been a recent body of work on this idea (Snell et al., 2024; Welleck et al., 2024; Muennighoff et al., 2025; Yeo et al., 2025), with OpenAI’s o1 (OpenAI, 2024) and DeepSeek R1 (Guo et al., 2025) demonstrating strong reasoning performance with consistent gains from scaling test-time compute. However, our understanding of the training data properties that support test-time scaling remains limited.

Training on diverse and difficult data has shown to be beneficial to enable test-time scaling on complex reasoning tasks, such as mathematical competitions (Muennighoff et al., 2025), medical reasoning (Huang et al., 2025b), and code (Yu et al., 2025). Difficult examples are often identified as those that cannot be answered by the model being trained or other more powerful proxy models. However, the precise notion of difficulty and the relation between the amount of compute at training and test time remains unclear. In particular,

- (i) Does increasing the test-time compute always improve the downstream reasoning performance?
- (ii) Can increasing the test-time compute lower the requirement on training-time compute?
- (iii) What are difficult training examples and why are they beneficial for test-time scaling? Addressing this question requires a rigorous understanding of the effect of training data and its properties on the performance of test-time scaling.

In this paper, we theoretically study the performance of test-time scaling for transformers trained on an in-context weight prediction task for linear regression, where the goal is to predict the linear weight vector from the sequence of input prompts. This framework has been used previously for analyzing

054 the mechanism underlying training CoT (Huang et al., 2025a). During training, the model performs  
 055 direct in-context-learning and outputs its prediction of the weight vector. At test time, the transformer  
 056 performs CoT and generates multiple intermediate steps before arriving at its final prediction of the  
 057 weight vector. Our analysis yields several intriguing findings: First, fixing the test error, by increasing  
 058 the test-time compute we can decrease the number of in-context examples (context length) in training  
 059 prompts. Second, if the skills needed to solve the downstream task (corresponding to directions in  
 060 the data covariance matrix) are not sufficiently represented in the training data, increasing test-time  
 061 compute can harm performance, effectively causing the model to *overthink*. Finally, we characterize  
 062 hardness of a task based on the smallest eigenvalue of its feature covariance matrix and show that  
 063 training on a diverse, relevant and hard set of tasks during training yields the best performance for  
 064 test-time scaling.

065 Our **main contributions** and the organization of the paper are discussed below:

066 (a) In Section 3, We study in-context learning in transformers with a single linear self-attention  
 067 (LSA) layer trained via gradient descent. Despite the problem’s non-convexity, we show that  
 068 gradient descent, when initialized randomly but suitably, converges to a global minimum, which  
 069 we explicitly characterize. Our analysis allows for general feature covariance. During training, the  
 070 model engages in direct in-context learning, but at test time we employ chain-of-thought (CoT)  
 071 prompting to let the model generate intermediate reasoning steps before producing its final output.  
 072 We demonstrate that, with CoT prompting at test time, the transformer effectively implements a  
 073 multi-step (pseudo-) Newton’s method for loss optimization. Notably, this part of our contribution  
 074 extends the results of Zhang et al. (2024) by incorporating CoT dynamics at test time, and of Huang  
 075 et al. (2025a) by accommodating general feature covariance.

076 (b) By analyzing the expected estimation error of in-context weights for test prompts, in Section 3.4 we  
 077 introduce a measure of task hardness defined by the ratio of the smallest eigenvalue of the feature  
 078 covariance matrix to its trace. We interpret the eigenvectors as representing different skills relevant  
 079 to the task, with the corresponding eigenvalues indicating the strength of those skills. Under this  
 080 interpretation, hard tasks are characterized by a long-tailed spectrum of skills, while easy tasks  
 081 correspond to having only a few well-balanced skills.

082 This analysis leads to two key consequences: (1) For a fixed test error, *increasing test-time compute*  
 083 *allows us to reduce the required number of in-context examples* (i.e., the context length) in training  
 084 prompts. (2) We derive **test-time scaling laws** for our ICL setting, capturing how test error depends  
 085 on test-time compute and highlighting the role of factors such as context length, feature dimension,  
 086 and task covariance structure in shaping the overall trend.

087 (c) In Section 5.1, we study a setting with  $T$  tasks, where each task is specified by its feature covariance  
 088 matrix (interpreted, as discussed in part (b), as the set of skills required for the task together  
 089 with their relative strengths). We extend the analysis of Section 3 to this multi-task setting and  
 090 characterize the estimation error of the final CoT output. Based on this characterization, we  
 091 formulate a quadratic optimization problem to determine the optimal task selection probabilities,  
 092 demonstrating that *training on a diverse, relevant, and sufficiently hard set of tasks yields the best*  
 093 *performance under test-time scaling*. We validate our theoretical results with experiments on both  
 094 Linear Self-Attention (LSA) models and the more complex nonlinear transformer architecture  
 095 GPT-2.

## 096 2 RELATED WORK

098 Recent work has highlighted several phenomena relevant to our study. First, it has been observed that  
 099 simply increasing test-time compute and reasoning depth can, counterintuitively, harm performance,  
 100 a phenomenon termed *overthinking*. The empirical study of Su et al. (2025) suggests that LLMs  
 101 tend to overthink simple problems by generating unnecessarily long outputs, and underthink harder  
 102 ones, by providing shallow or incomplete reasoning that overlooks critical steps. In Wang et al.  
 103 (2025), it is argued that exploring more reasoning branches may degrade system efficiency as many  
 104 branches may be trapped in overthinking. Second, Recent work has explored the test-time scaling  
 105 paradigm (Snell et al., 2024; Welleck et al., 2024), with OpenAI’s o1 (OpenAI, 2024) and DeepSeek  
 106 R1 (Guo et al., 2025) demonstrating strong performance through reinforcement learning on millions  
 107 of samples and multiple training stages. Muennighoff et al. (2025) proposes a simple framework,  
 which involves training on only 1,000 samples with next-token prediction and controlling thinking

duration via a simple test-time technique, and show that it achieves test-time scaling and strong reasoning performance. Finally, prior studies on data mixtures emphasize the importance of balancing training corpora with sufficient coverage of topics matched to downstream tasks, as imbalanced data composition can impair generalization (Xie et al., 2023; Nguyen et al., 2024). However, prior work has been largely empirical, whereas we develop a theoretical framework that rigorously analyzes test-time scaling and Chain-of-Thought effectiveness, overthinking, and principled strategies for task selection during training.

### 3 IN-CONTEXT LEARNING

In an in-context learning (ICL) scenario, a model is presented with instances of prompts of the form  $P_\tau = (x_1, h_\tau(x_1), \dots, x_n, h_\tau(x_n))$ , with  $x_i$  drawn i.i.d from a distribution  $\mathcal{D}_x$ , and  $h_\tau$  sampled independently from a distribution over functions in a given function class. The goal of in-context learning is to train a model so that when given a test prompt  $P_{\tau'} = (x_1, h_{\tau'}(x_1), \dots, x_m, h_{\tau'}(x_m), x_{m+1})$  with an independently sampled  $h_{\tau'}$ , it is able to make a prediction on  $x_{m+1}$  that is close to  $h_{\tau'}(x_{m+1})$ . Therefore, a key distinction from traditional supervised learning is that in ICL, each prompt has its own distribution. For example, in linear regression,  $h_\tau(x) = \langle w_\tau, x \rangle$ , where each prompt has its own ground truth  $w_\tau$ . Thus, in ICL the model must generalize not just across data points but across distributions, and be able to infer the correct predictive rule on the fly for each new prompt without modifying its parameters.

#### 3.1 IN-CONTEXT WEIGHT PREDICTION AND LINEAR SELF-ATTENTION

We focus on ICL for linear regression task, where each prompt  $P_\tau = (x_{\tau,1}, y_{\tau,1}, \dots, x_{\tau,n}, y_{\tau,n})$  with  $y_\tau = \langle w_\tau, x_{\tau,i} \rangle$ , where  $x_{\tau,i} \sim N(0, \Lambda)$ ,  $w_\tau \sim N(0, I_d)$ . Most previous works on this setting focus on prediction without directly estimating the weight vector of the test prompt (Ahn et al., 2023a; Zhang et al., 2024; Mahankali et al., 2023). Here, we take a similar approach to Huang et al. (2025a) and consider in-context weight prediction where we require the model to directly estimate the weight vector of test prompts. To this end, we adopt the embedding used by Bai et al. (2023); Huang et al. (2025a) which includes the weight-estimation:

$$E_\tau = \begin{bmatrix} x_{\tau,1} & \dots & x_{\tau,n} & 0 \\ y_{\tau,1} & \dots & y_{\tau,n} & 0 \\ 0 & \dots & 0 & \hat{w}_0 \\ 0 & \dots & 0 & 1 \end{bmatrix} := \begin{bmatrix} X_\tau & 0 \\ y_\tau & 0 \\ 0_{d \times n} & \hat{w}_0 \\ 0_{1 \times n} & 1 \end{bmatrix} \quad (3.1)$$

where  $\hat{w}_0 \in \mathbb{R}^d$  is an initialization for the weight estimate.

We next proceed by describing the transformer architecture. We consider a one layer self-attention with residual connection. Let  $E$  be an embedding formed from the prompt. A self-attention module takes as input an embedding matrix and outputs a matrix of the same size,

$$f_{\text{Attn}}(E; W_K, W_Q, W_V, W_P) = E + W_P W_V E \cdot \psi \left( \frac{(W_K E)^\top W_Q E}{\rho} \right)$$

where  $\psi$  is an activation (e.g. softmax) that is applied column-wise. Following Gatmiry et al. (2024); Huang et al. (2025a); Zhang et al. (2024); Ahn et al. (2023b), we consider Linear-Self-Attention (LSA) where the activation  $\psi$  is the identity mapping. By defining  $W := W_K^\top W_Q$ ,  $V = W_P W_V$  and  $\theta = (W, V)$  we arrive at

$$f_{\text{LSA}}(E; \theta) = E + V E \cdot \frac{E^\top W E}{\rho}. \quad (3.2)$$

The estimation of the transformer for  $w_\tau$  is given by the last token of the output sequence, namely  $\hat{w}_\tau = f_{\text{LSA}}(E_\tau; \theta)_{[d+2:2d+1, -1]}$ , which is obtained by restricting the last column of  $f_{\text{LSA}}(E_\tau; \theta)$  to entries  $[d+2 : 2d+1]$ . We assume  $\hat{w}_0 = 0$  for simplicity.

We learn the parameters of the transformer by minimizing the following empirical loss over  $B$  independent prompts:

$$\hat{L}(\theta) = \frac{1}{2B} \sum_{\tau=1}^B \|f_{\text{LSA}}(E_\tau; \theta)_{[:, -1]} - (0_d, 0, w_\tau, 1)\|_{\ell_2}^2 \quad (3.3)$$

162 We consider the behavior of gradient descent-trained networks over the population loss induced by  
 163 the limit of infinite training prompts:

$$165 \quad L(\theta) = \lim_{B \rightarrow \infty} \widehat{L}(\theta) = \frac{1}{2} \mathbb{E}_{w_\tau, x_{\tau,1}, \dots, x_{\tau,n}} \left( \|f_{\text{LSA}}(E_0; \theta)_{[:, -1]} - (0_d, 0, w_\tau, 1)\|_{\ell_2}^2 \right) \quad (3.4)$$

166 Our first result shows that with suitable initialization and step size, gradient descent converges to a  
 167 global minimum of  $L(\theta)$ , which we explicitly characterize.

169 **Theorem 3.1** *Consider the linear self-attention network over the population loss (3.4) with initial-  
 170 ization*

$$171 \quad V(0) = \begin{bmatrix} 0 & 0 & 0 & 0 \\ 0 & 0 & 0 & 0 \\ V_{31}(0) & 0 & 0 & 0 \\ 0 & 0 & 0 & 0 \end{bmatrix}, \quad W(0) = \begin{bmatrix} 0 & 0 & cI & 0 \\ 0 & 0 & 0 & -c \\ 0 & 0 & 0 & 0 \\ 0 & 0 & 0 & 0 \end{bmatrix}$$

174 for some real-valued  $c$ . Also define

$$175 \quad \Gamma := \left(1 + \frac{1}{n}\right) \Lambda + \frac{1}{n} \text{tr}(\Lambda) I_d \in \mathbb{R}^{d \times d}. \quad (3.5)$$

178 We run gradient descent on the population loss with constant step size  $\eta \leq 1/(c^2 \|\Gamma\|_{\text{op}})$ . We also fix  
 179  $W_{24}(t) = -c$ . The gradient descent converges to a global minimum of the loss given by

$$180 \quad V_* = \begin{bmatrix} 0 & 0 & 0 & 0 \\ 0 & 0 & 0 & 0 \\ -\frac{\Gamma^{-1}}{c} & 0 & 0 & 0 \\ 0 & 0 & 0 & 0 \end{bmatrix}, \quad W_* = \begin{bmatrix} 0 & 0 & cI & 0 \\ 0 & 0 & 0 & -c \\ 0 & 0 & 0 & 0 \\ 0 & 0 & 0 & 0 \end{bmatrix}. \quad (3.6)$$

185 Note that chain-of-thought reasoning is not employed during training; however, as we discuss in  
 186 the following section, the model engages in chain-of-thought reasoning at test time. In contrast,  
 187 (Huang et al., 2025a, Theorem 3.1) consider the setting of isotropic Gaussian features ( $\Lambda = I$ ) and  
 188 incorporate chain-of-thought reasoning during training by generating intermediate steps through  
 189 gradient updates on the linear regression objective. Also, the result of (Zhang et al., 2024, Theorem  
 190 4.1) does not apply to our setting, since it works with a different embedding and trains the model by  
 191 minimizing the expected prediction loss function.

### 192 3.2 TEST TIME CHAIN-OF-THOUGHT

194 During test time, we observe a test prompt of the form  $P = (x_1, \langle w_{\text{test}}, x_1 \rangle, \dots, x_m, \langle w_{\text{test}}, x_m \rangle)$   
 195 of possibly different length than the training prompts, and  $w_{\text{test}}$  may be never seen before. We  
 196 let the transformer to generate  $k$  steps before it outputs the final prediction  $w_k$  of the ground  
 197 truth  $w_{\text{test}}$ . Specifically, we let  $E_i$  be the embedding at the  $i$ -th step of generation, and have  
 198  $f_{\text{LSA}}(E_i)[d+2 : 2d+1, -1]$  as the prediction of the next link in the chain. We then append it to the  
 199 current embedding, as follows:

$$201 \quad E_i = \begin{bmatrix} x_1 & \dots & x_m & 0 & 0 & \dots & 0 \\ y_1 & \dots & y_m & 0 & 0 & \dots & 0 \\ 0 & \dots & 0 & w_0 & w_1 & \dots & w_i \\ 0 & \dots & 0 & 1 & 1 & \dots & 1 \end{bmatrix} := \begin{bmatrix} X_{\text{test}} & 0 & 0 & \dots & 0 \\ y_{\text{test}} & 0 & 0 & \dots & 0 \\ 0_{d \times n} & w_0 & w_1 & \dots & w_i \\ 0_{1 \times n} & 1 & 1 & \dots & 1 \end{bmatrix} \quad (3.7)$$

205 with  $w_i := f_{\text{LSA}}(E_{i-1})[d+2 : 2d+1, -1]$ . The final prediction is given by  $w_{k+1}$ . In our next proposition,  
 206 we give an explicit characterization of the recursive updates of  $w_i$ .

207 **Proposition 3.2** *Consider the LSA model with parameters  $V_*$  and  $W_*$  given by (3.6) and assume  
 208 a test prompt of the form  $P = (x_1, \langle w_{\text{test}}, x_1 \rangle, \dots, x_m, \langle w_{\text{test}}, x_m \rangle)$ . Initializing the test time CoT  
 209 with  $w_0 = 0$ , we have*

$$210 \quad w_{i+1} = w_i - \frac{1}{m} \Gamma^{-1} X_{\text{test}} X_{\text{test}}^\top (w_i - w_{\text{test}}), \quad (3.8)$$

212 where  $X_{\text{test}} = [x_1 | \dots | x_m] \in \mathbb{R}^{d \times m}$ . Therefore, the final output (after  $k$  step of generation) is given  
 213 by

$$214 \quad w_{k+1} = \left( I - \left( I - \frac{1}{m} \Gamma^{-1} X_{\text{test}} X_{\text{test}}^\top \right)^k \right) w_{\text{test}}. \quad (3.9)$$

216 **Remark 3.3** Consider the quadratic loss  $\ell(w) := \frac{1}{2m} \|y_{\text{test}} - X_{\text{test}}^T w\|_{\ell_2}^2$ , with  $y_{\text{test}} = X_{\text{test}}^T w_{\text{test}}$ .  
 217 The gradient of the loss is given by  $\nabla \ell(w) = -\frac{1}{m} X_{\text{test}}(y_{\text{test}} - X_{\text{test}}^T w) = \frac{1}{m} X_{\text{test}} X_{\text{test}}^T (w - w_{\text{test}})$ ,  
 218 and the expected Hessian is given by  $\mathbb{E}[\nabla^2 \ell(w)] = \mathbb{E}[\frac{1}{m} X_{\text{test}} X_{\text{test}}^T] = \Lambda$ . Treating  $\Gamma$ , given by (3.5),  
 219 as a regularized form of  $\Lambda$ , the update (3.8) is (pseudo-) Newton's method for optimizing the loss.  
 220

221 **3.4 HARDNESS OF A TASK**  
 222

223 We define a task by the covariance matrix of its features ( $\Lambda$ ), so different tasks have different features  
 224 covariances and for each task, we have many prompts with features generated from  $\mathcal{N}(0, \Lambda)$ , but each  
 225 with its own  $w_\tau$ . Now suppose we perform direct in-context learning on a task and then use it to  
 226 predict labels on queries from the same task (without CoT). Our next result will bound the expected  
 227 estimation error and we use that to define a measure of task hardness.  
 228

229 **Theorem 3.3** Consider the LSA model with parameters  $V_*$  and  $W_*$  and assume a test prompt is of the  
 230 form  $P = (x_1, \langle w_{\text{test}}, x_1 \rangle, \dots, x_m, \langle w_{\text{test}}, x_m \rangle)$ . Initializing the in-context learning with  $w_0 = 0$ ,  
 231 the estimate of  $w$  will be given by  $\hat{w} = \frac{1}{n} \Gamma^{-1} X_{\text{test}} X_{\text{test}}^T w$  with  $X_{\text{test}} = [x_1 | \dots | x_m] \in \mathbb{R}^{d \times m}$ . We  
 232 have

$$233 \mathbb{E}_{X_{\text{test}}} (\|\hat{w} - w_{\text{test}}\|^2) \leq w_{\text{test}}^T \left( \frac{1}{n^2} (I + \text{tr}(\Lambda) \Lambda^{-1})^2 + \frac{1}{m} (I + \text{tr}(\Lambda^{-1}) \Lambda) \right) w_{\text{test}} \\ 234$$

235 where the expectation is with respect to  $X_{\text{test}}$ . Taking expectation with respect to  $w_{\text{test}} \sim \mathcal{N}(0, I)$ ,  
 236 we obtain

$$237 \mathbb{E}(\|\hat{w} - w_{\text{test}}\|^2) \leq \frac{d}{n^2} \left( 1 + \frac{\text{tr}(\Lambda)}{\lambda_{\min}(\Lambda)} \right)^2 + \frac{d}{m} \left( 1 + \frac{\text{tr}(\Lambda)}{\lambda_{\min}(\Lambda)} \right). \quad (3.10) \\ 238 \\ 239$$

240 Based on the above result, we define the hardness of a task, with features covariance  $\Lambda$ , via the  
 241 following measure:

$$242 \text{Hard}(\Lambda) := \frac{\text{tr}(\Lambda)}{\lambda_{\min}(\Lambda)}. \quad (3.11) \\ 243 \\ 244$$

245 Note that it is invariant to scaling of  $\Lambda$  and would be higher if  $\Lambda$  has some small eigenvalue as more  
 246 data is needed to learn these directions. Our next results bound the expected estimation error under  
 247 CoT during test time.

248 **Theorem 3.4** Consider the setting of Theorem 3.3 and let  $w_{k+1}$  be the model estimate for the target  
 249 task after generating  $k$  steps during test time. Also suppose that  $m = \Omega(k^2 d)$  and that eigenvalues of  
 250  $\Lambda$  are upper and lower bounded by positive constants. We have

$$251 \mathbb{E}(\|w_{k+1} - w_{\text{test}}\|_{\ell_2}^2) \leq \text{tr}((I - \Gamma^{-1} \Lambda)^{2k}) (1 + O(k \sqrt{d/m})) \\ 252$$

253 where the expectation is with respect to  $X_{\text{test}} = [x_1 | \dots | x_m]$  and  $w_{\text{test}} \sim \mathcal{N}(0, I)$ .  
 254

255 **Corollary 3.5** Under the setting of Theorem 3.4, and letting  $\lambda_{\min}(\Lambda) > 0$  be the minimum eigenvalue  
 256 of  $\Lambda$  we have

$$257 \mathbb{E}(\|w_{k+1} - w_{\text{test}}\|_{\ell_2}^2) \leq d \left( 1 + \frac{n}{1 + \text{Hard}(\Lambda)} \right)^{-2k} (1 + o(1)). \\ 258$$

259 The above corollary is also consistent with our measure of hardness: the estimation error of  $w_{k+1}$   
 260 increases with  $\text{Hard}(\Lambda)$ . In addition, if we want to get the estimation error below some target level  $\varepsilon$ ,  
 261 harder tasks require longer CoT at test time (larger  $k$ ).

262 Note that in Corollary 3.5, it was assumed that  $\Lambda$  is full rank. If  $\Lambda$  is rank deficient (that is the  
 263 features are coming from a subspace of lower dimension), then one cannot estimate  $w_{\text{test}}$  along those  
 264 directions, as we do not see any information about them during the process. This of course is not  
 265 an issue if the prompts during test time are coming from the same task, as those directions do not  
 266 contribute to the predictions. In these cases, by restricting to the relevant subspace, hardness of the  
 267 task can be defined similarly where  $\lambda_{\min}(\Lambda)$  is the minimum “non-zero” eigenvalue of  $\Lambda$ .  
 268

An interpretation of the hardness measure is that each eigenvector of  $\Lambda$  corresponds to a specific skill needed for solving examples from that task, with the corresponding eigenvalues indicating the strength of those skills. An easy task is one that relies on a few dominant skills (a small number of nonzero eigenvalues of similar magnitude), while a hard task draws on many skills, reflected in a long-tailed spectrum. The proposed measure captures this intuition quantitatively.

**Remark 3.5 Test-time scaling.** Our result in Corollary 3.5 provides test time scaling for our ICL setting. Note that the computational complexity during test time increases as we allow for more steps of thinking; Specifically, it is  $O(kd^2)$  as the matrix  $I - \frac{1}{m}\Gamma^{-1}X_{\text{test}}X_{\text{test}}^\top$  can be computed once, and each step of thinking involves multiplying it with the current estimate. Our result also captures the role of  $\lambda_{\min}$ ,  $\text{tr}(\Lambda)$  and the prompts length  $n$  during training and the features dimension  $d$  in shaping the test time scaling law. Another observation is that at any fixed test error, by increasing  $k$  we can decrease the length of prompts during training. In Figure 1, we illustrate test-time scaling for several choices of prompt lengths ( $n$ ) and task hardness.

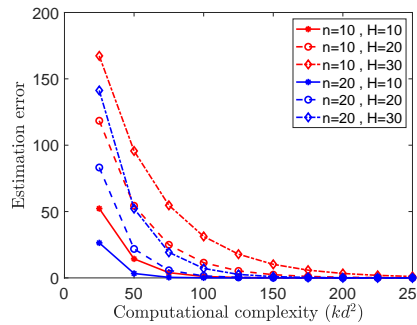


Figure 1: Test-time scaling for the in-context learning. Here,  $n$  is the number of in-context examples (context length) in training prompts, and  $H$  is the task hardness.

## 4 TASK SELECTION FOR TRAINING

We consider a set of  $T$  tasks with corresponding covariances  $\Lambda_1, \dots, \Lambda_T$ . Similar to previous sections we draw infinite prompts ( $B \rightarrow \infty$ ) but here each prompt is selected from task  $i$  with probability  $\pi_i \geq 0$ , where  $\sum_i \pi_i = 1$ . The goal of this section is to derive optimal choice of  $\{\pi_i\}_{i=1}^T$  and build insights about this choice.

**Theorem 4.1** Consider the linear self-attention network and the population loss (3.4) under the multi-task setting, with the same initialization given in Theorem 3.1. Redefine  $\Gamma$  as follows:

$$\Gamma := \frac{n-1}{n} \sum_{\ell \in [T]} \Lambda_\ell \pi_\ell + \frac{1}{n} \left( 2 \sum_{\ell \in [T]} \Lambda_\ell^2 \pi_\ell + \sum_{\ell \in [T]} \text{tr}(\Lambda_\ell) \Lambda_\ell \pi_\ell \right) \left( \sum_{\ell \in [T]} \Lambda_\ell \pi_\ell \right)^{-1}. \quad (4.1)$$

Then a similar statement to Theorem 3.1 holds true.

We next consider a target task with covariance  $\Sigma$  (which can be different from any of the tasks during training). For a prompt from it,  $P = (x_1, \langle w_{\text{test}}, x_1 \rangle, \dots, x_m, \langle w_{\text{test}}, x_m \rangle)$ , we let  $X_{\text{test}} = [x_1 | \dots | x_m] \in \mathbb{R}^{d \times m}$  and  $\widehat{\Sigma} := \frac{1}{m} X_{\text{test}} X_{\text{test}}^\top$ . Initializing with  $w_0 = 0$  and allowing for a chain-of-thought of length  $k$ , the LSA estimate of  $w_{\text{test}}$  reads  $w_{k+1} = (I - \Gamma^{-1} \widehat{\Sigma})^k w_{\text{test}}$ . Therefore,

$$\mathbb{E}(\|w_{k+1} - w_{\text{test}}\|^2) = \mathbb{E}(\|(I - \Gamma^{-1} \widehat{\Sigma})^k w_{\text{test}}\|^2) = \mathbb{E}[\text{tr}((I - \widehat{\Sigma} \Gamma^{-1})^k (I - \Gamma^{-1} \widehat{\Sigma})^k)], \quad (4.2)$$

where the second step is by taking expectation with respect to  $w_{\text{test}}$ . In the next proposition, we derive a *prompt instance independent* upper bound for the estimation error in terms of the population covariance  $\Sigma$ .

**Proposition 4.2** Suppose that  $m = \Omega(k^2 d)$ . Then,

$$\mathbb{E}[\text{tr}((I - \widehat{\Sigma} \Gamma^{-1})^k (I - \Gamma^{-1} \widehat{\Sigma})^k)] \leq \text{tr}(\Gamma) \text{tr}(\Gamma^{-1}) \text{tr}((I - \Gamma^{-1/2} \Sigma \Gamma^{-1/2})^{2k}) (1 + o(1)). \quad (4.3)$$

The optimal choice of tasks selection probabilities is the one that minimizes the expected estimation error during test time given by (4.2). We instead use the upper bound given by Proposition 4.2 and focus on the term  $\text{tr}((I - \Gamma^{-1/2}\Sigma\Gamma^{-1/2})^{2k})$  in (4.3), which captures the effect of thinking and is the dominant term with an exponential rate. This results in the following optimization for choosing task selection probabilities:

$$\begin{aligned} \min_{\pi_\ell, \ell \in [m]} \quad & \mathbb{E}[\text{tr}((I - \Gamma^{-1/2}\Sigma\Gamma^{-1/2})^{2k})] \\ \text{subject to} \quad & \sum_{\ell \in [T]} \pi_\ell = 1, \quad \pi_\ell \geq 0, \quad \forall \ell \in [T] \end{aligned} \quad (4.4)$$

**Remark 4.1 When is the test time thinking useful?** We observe that the effect of thinking at inference time is captured by the term  $\text{tr}((I - \Gamma^{-1/2}\Sigma\Gamma^{-1/2})^{2k})$ . Depending on the eigenvalues of  $\Gamma^{-1/2}\Sigma\Gamma^{-1/2}$ , this term may shrink or grow as  $k$  increases. Intuitively, if each eigenvector of  $\Sigma$  (representing the skills required at test time) is sufficiently represented in the training data—so that  $\Gamma$  is strong along that direction and  $\Gamma^{-1/2}\Sigma\Gamma^{-1/2}$  remains small—then additional thinking improves performance. In contrast, if some task-relevant directions are underrepresented in the training data, and thus not well learned by the model, increasing the amount of test-time thinking can degrade performance, effectively leading to overthinking.

## 4.2 OPTIMAL CHOICE OF TASK SELECTION PROBABILITIES

We next analyze the optimization (4.4) to argue that choosing a diverse, relevant and hard set of tasks during training results in best performance for test-time scaling.

**Diversity.** A key observation is that we must select a *diverse* set of tasks so that the spectrum of  $\Gamma$  adequately covers all directions in the target covariance  $\Sigma$ . Failing to do so causes  $\Gamma^{-1/2}\Sigma\Gamma^{-1/2}$  to be large along uncovered directions, resulting in higher test error that may further amplify with additional reasoning steps.

**Relevance.** Another important notion is the *relevance* of the selected tasks to the target task. Recall the expression of  $\Gamma$  given by (4.1). When  $d \ll n$ , and noting that the eigenvalues of  $\Lambda$  are  $O(1)$ ,  $\Gamma$  can be replaced by  $\tilde{\Gamma} := \sum_{\ell \in [T]} \Lambda_\ell \pi_\ell$ , which is a convex combination of  $\{\Lambda_\ell\}_{\ell \in [m]}$ . Hence, minimizing  $\text{tr}((I - \Gamma^{-1/2}\Sigma\Gamma^{-1/2})^{2k})$  in effect corresponds to approximating  $\Sigma$  with a convex combination of the task covariance matrices and so tasks which place high weight on directions well represented in  $\Sigma$  (i.e. relevant ones) are desirable.

**Hardness.** The other factor in task selection is the hardness of tasks. We argue that when the target task is hard (as is often the case where models are compared on difficult benchmarks), our proposal favors selecting hard tasks during training. Without loss of generality, by scaling features we can assume that  $\text{tr}(\Lambda_\ell) = 1, \forall \ell$  and  $\text{tr}(\Sigma) = 1$ . With this normalization the hardness of task is captured by the minimum eigenvalue of the corresponding covariance matrix. Now, invoking the test error given by  $\text{tr}((I - \Gamma^{-1/2}\Sigma\Gamma^{-1/2}))$ , the absolute error along minimum eigenvectors of  $\Sigma$  contribute more towards the error. Given that the target task is a hard one,  $\sigma_{\min}(\Sigma)$  is small and in the next proposition we show that to estimate  $\Sigma$  well on this direction by a convex combination of available tasks, we need to select some hard tasks (those with small minimum eigenvalue).

**Proposition 4.3** Suppose that  $|\sigma_{\min}(\Gamma) - \sigma_{\min}(\Sigma)| \leq \varepsilon$  and define  $D := \{\ell \in [T], \sigma_{\min}(\Lambda_\ell) \leq 4(\varepsilon + \sigma_{\min}(\Sigma))\}$ . Note that  $D$  corresponds to tasks with small minimum eigenvalues (hard tasks), since both  $\varepsilon$  and  $\sigma_{\min}(\Sigma)$  are small. Then,  $\sum_{\ell \in D} \pi_\ell \geq 1/2$ . In words, at least 1/2 of task selection probabilities are on hard tasks.

**Further simplification of task selection procedure.** Note that the optimization problem (4.4) is inherently nonconvex, which motivates us to turn to simplifications that transform it into a convex and tractable form for large-scale problems. We make two modifications: 1) As discussed before when  $d \ll n$  and since the the eigenvalues of  $\Lambda$  are  $O(1)$ ,  $\Gamma$  can be well approximated by  $\tilde{\Gamma} := \sum_{\ell \in [T]} \Lambda_\ell \pi_\ell$ , which is a convex combination of  $\{\Lambda_\ell\}_{\ell \in [m]}$ . 2) The objective in (4.4) seeks to make  $\Gamma^{-1/2}\Sigma\Gamma^{-1/2}$  close to the identity matrix. Instead, we minimize  $\|I - \Sigma^{-1}\Gamma\|_F^2 \approx \|I - \Sigma^{-1}\tilde{\Gamma}\|_F^2$ , which pursues the same goal but through a different formulation. With these consideration, we propose the following

378 alternative optimization for choosing task selection probabilities  $\{\pi_\ell\}_{\ell \in [T]}$ :  
 379

$$\begin{aligned} 380 \quad & \min_{\{\pi_\ell\}_{\ell \in [T]}} \quad \left\| I - \Sigma^{-1} \sum_{\ell \in [T]} \Lambda_\ell \pi_\ell \right\|_F^2 \\ 381 \quad & \text{subject to } \sum_{\ell \in [T]} \pi_\ell = 1, \quad \pi_\ell \geq 0, \quad \forall \ell \in [T] \\ 382 \quad & \\ 383 \quad & \\ 384 \quad & \\ 385 \quad & \end{aligned} \tag{4.5}$$

386 This is a quadratic optimization problem and can be efficiently solved at scale.  
 387

## 388 5 EXPERIMENTS

391 In this section, we conduct experiments to validate our theoretical results.  
 392

393 **Setting.** We conduct experiments in two settings. First, we consider a transformer with a single  
 394 linear self-attention (LSA) to confirm our theory. Then, we consider large, nonlinear transformer  
 395 architecture namely GPT2 to validate our conclusions. In both cases, the data distribution follows  
 396 our in-context weight prediction task in Sec. 3.1, where  $x_{\tau,i} \sim \mathcal{N}(0, \Lambda)$ ,  $w_\tau \sim \mathcal{N}(0, I_d)$ . We choose  
 397 the token dimensions  $d = 10$ . During inference, we let the model to output multiple steps before  
 398 returning the final predicted weight vector. At each step  $i$  we concatenate the embedding with  
 399  $[0_d, \hat{w}_i, 1]$  as in Eq. (3.7) and input the concatenated embedding matrix to the model. The predicted  
 400  $w_k$  will be returned after  $k$  steps of CoT. We report the average results and error bars over 10 runs.  
 401

402 **Transformers with a single linear self-attention (LSA).** We train the transformer architecture in Eq.  
 403 (3.2) on the synthetic data generated as described above. We generate 5000 examples, use a batch size  
 404  $B = 1000$  and run Adam with learning rate  $\eta = 0.001$  for  $= 1000$  epochs. For the results reported in  
 405 the main paper we follow our theoretical setting in Sec. 3.1. **That is, we initialize transformer weights**  
 406 **( $V(0), W(0)$ ) according to Theorem 3.1 where  $V31(0)$  is set randomly with entries independently**  
 407 **and uniformly drawn from  $[0, 1]$ , and we set  $c = 1$ . We also do not perform CoT during training.**  
 408

409 We report additional results with random initialization and training with CoT in Appendix B.  
 410

411 **Large, nonlinear transformer architectures.** We use a decoder-only Transformer architecture  
 412 (Vaswani et al., 2017) from the GPT-2 family (Radford et al., 2019), consisting of 12 layers, 8 attention  
 413 heads, and a 256-dimensional embedding space. In total the model contains 9.5M parameters.  
 414

415 This architecture takes as input a sequence of vectors in its embedding space and predicts  
 416 the weight vector within the same space. We apply this architecture to prompts of form  
 417  $(x_{\tau,1}, y_{\tau,1}, \dots, x_{\tau,m}, y_{\tau,m}, w_0, 1)$  in the following manner. In line with (Garg et al., 2022), we  
 418 map each  $y_{\tau,i}$  to the same dimension as  $x_{\tau,i}$  by appending zeros, and map  $x_{\tau,i}, y_{\tau,i}$  into the latent  
 419 embedding space of the Transformer through a (learnable) linear transformation. We get the predicted  
 420  $w_\tau$  as the model output. **Similarly, we map the model output, i.e.,  $w_\tau$  from the latent embedding**  
 421 **space of the Transformer to a  $d$ -dimensional vector through another (learnable) linear transformation.**  
 422 Training is performed with a batch size of 64 over  $25k$  total steps. The model is randomly initialized,  
 423 and CoT is applied during both training and inference. **We used curriculum learning Garg et al. (2022)**  
 424 **to speed up training.**

425 **Larger test-time compute reduces the requirement on training-time compute.** Fig 2a, 2c show  
 426 test error vs length of CoT ( $k$ ). For the LSA model, we use  $n = 10, 20, 30$  and for GPT-2 we use  
 427  $n = 20, 30, 40$ . We see that by increasing the test-time compute ( $k$ ), we can decrease the length of  
 428 prompts  $n$  during training to get a similar test error.  
 429

430 **When more thinking hurts.** For training, we sample prompt inputs from  $\mathcal{N}(0, \Lambda)$  where  $\Lambda$  is a skewed  
 431 covariance matrix with eigenbasis chosen uniformly at random and  $i$ -th eigenvalue proportional to  
 432  $1/i$ . For test, we sample prompt inputs from  $\mathcal{N}(0, I_d)$ . We normalize the inputs so that their expected  
 433 squared norm is equal to that of inputs encountered during training. Fig 2b, 2d show that when some  
 434 of the directions of the target task are not sufficiently present in the training data, allowing for more  
 435 thinking during test time would hurt the performance. An interesting observation is that when the  
 436 model is in overthinking regime (Fig 2b, 2d) larger prompt length  $n$  yields a higher test loss, while  
 437 when the model is not overthinking, larger  $n$  reduces the test loss (Fig 2a, 2c).  
 438

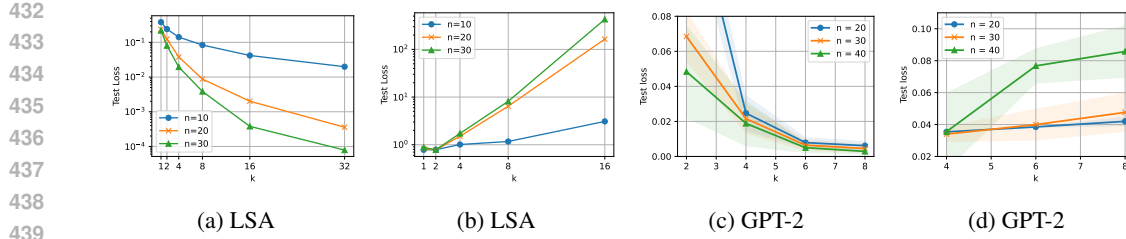


Figure 2: More test-time compute reduces training-time requirements for (a) one-layer transformer and (c) GPT-2. However, insufficient task coverage in training data makes longer CoTs harmful for (b) one-layer transformer and (d) GPT-2. For GPT-2, the errorbars are std of 10 runs. For LSA, std is negligible as we start from the fixed initialization in Eq. (3.6). [Same value for  \$n\$  is used in training and test.](#)

### 5.1 TASK SELECTION

We design an experiment to illustrate that our method prioritizes diverse and hard tasks. We consider a multi-task setup with four task types, where each type is defined by two parameters  $\alpha$  and  $B$ . These parameters respectively control the decay rate and the support size of the eigenvalues. Specifically, eigenvalues are proportional to  $i^{-\alpha}$  for  $i \in [B]$  and zero elsewhere. The positions of nonzero eigenvalues are uniformly shuffled within  $[d]$ , and the eigenvalues are scaled to have unit sum. Here,  $B$  captures task diversity, while  $\alpha$  captures the task hardness (with larger  $\alpha$  producing smaller nonzero eigenvalues, corresponding to harder tasks according to measure (3.11)).

The four training task types are: Easy-Short ( $\alpha = 0.2, B = 20$ ), Hard-Short ( $\alpha = 0.8, B = 20$ ), Easy-Long ( $\alpha = 0.2, B = 100$ ), and Hard-Long ( $\alpha = 0.8, B = 100$ ). The target task is set with  $\alpha = 0.8$  and  $B = d = 1000$ . We generate 50 tasks of each type by randomizing the eigenbases and the support of eigenvalues. We then solve the quadratic optimization problem (4.5) to obtain task selection probabilities  $\pi_\ell$ , for  $\ell = 1, \dots, 200$ . Fig 3a displays these probabilities, colored by task type, with solid lines indicating their average per type. As shown, harder and more diverse tasks receive higher selection probabilities, while easier, more concentrated tasks are weighted lower. Fig 3b further plots selection probability versus task hardness, confirming that harder tasks are indeed favored, consistent with our theoretical analysis in Section 5.1.

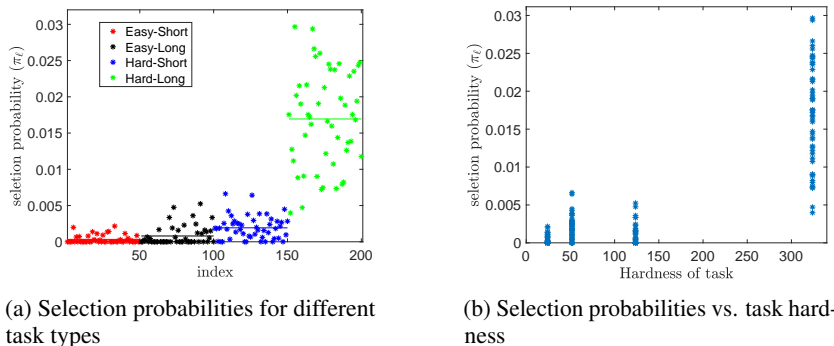


Figure 3: Task selection in a multi-task setup (a) Each color corresponds to a task type with solid lines indicating the average selection probability per type. As we observe harder and more diverse tasks receive higher selection probabilities, while easier, more concentrated tasks are weighted lower (b) Task selection probabilities versus task hardness. As we see harder task are favored in the selection.

## 6 CONCLUSION

In this work, we provided a theoretical and empirical framework for understanding in-context learning in transformers, showing that chain-of-thought prompting at test time enables models to emulate multi step (pseudo)-Newton's method. By introducing a principled notion of task hardness based on features covariance spectrum, we derived scaling laws that clarify how test-time compute, context

length, and task diversity interact. We proposed an optimal strategy for task selection in a multi-task training that shows training on a diverse, relevant and hard set of tasks during training results in best performance for test-time scaling. We also validated our findings on both linear self-attention models and GPT-2. We will conclude by discussing some limitations of our work which pave the way for future directions of work. Our theoretical analysis in this work is limited to linear regression tasks and single-layer linear self-attention, and an important direction for future work is extending these results to nonlinear data generation settings and transformers with nonlinear activations.

## REFERENCES

Kwangjun Ahn, Xiang Cheng, Hadi Daneshmand, and Suvrit Sra. Transformers learn to implement preconditioned gradient descent for in-context learning. *Advances in Neural Information Processing Systems*, 36:45614–45650, 2023a.

Kwangjun Ahn, Xiang Cheng, Minhak Song, Chulhee Yun, Ali Jadbabaie, and Suvrit Sra. Linear attention is (maybe) all you need (to understand transformer optimization). *arXiv preprint arXiv:2310.01082*, 2023b.

Yu Bai, Fan Chen, Huan Wang, Caiming Xiong, and Song Mei. Transformers as statisticians: Provable in-context learning with in-context algorithm selection. *Advances in neural information processing systems*, 36:57125–57211, 2023.

Shivam Garg, Dimitris Tsipras, Percy S Liang, and Gregory Valiant. What can transformers learn in-context? a case study of simple function classes. *Advances in neural information processing systems*, 35:30583–30598, 2022.

Khashayar Gatmiry, Nikunj Saunshi, Sashank J Reddi, Stefanie Jegelka, and Sanjiv Kumar. Can looped transformers learn to implement multi-step gradient descent for in-context learning? *arXiv preprint arXiv:2410.08292*, 2024.

Daya Guo, Dejian Yang, Haowei Zhang, Junxiao Song, Ruoyu Zhang, Runxin Xu, Qihao Zhu, Shirong Ma, Peiyi Wang, Xiao Bi, et al. Deepseek-r1: Incentivizing reasoning capability in llms via reinforcement learning. *arXiv preprint arXiv:2501.12948*, 2025.

Roger A Horn and Charles R Johnson. *Topics in matrix analysis*. Cambridge university press, 1994.

Jianhao Huang, Zixuan Wang, and Jason D Lee. Transformers learn to implement multi-step gradient descent with chain of thought. *arXiv preprint arXiv:2502.21212*, 2025a.

Xiaoke Huang, Juncheng Wu, Hui Liu, Xianfeng Tang, and Yuyin Zhou. m1: Unleash the potential of test-time scaling for medical reasoning with large language models. *arXiv preprint arXiv:2504.00869*, 2025b.

Arvind Mahankali, Tatsunori B Hashimoto, and Tengyu Ma. One step of gradient descent is provably the optimal in-context learner with one layer of linear self-attention. *arXiv preprint arXiv:2307.03576*, 2023.

Niklas Muennighoff, Zitong Yang, Weijia Shi, Xiang Lisa Li, Li Fei-Fei, Hannaneh Hajishirzi, Luke Zettlemoyer, Percy Liang, Emmanuel Candès, and Tatsunori Hashimoto. s1: Simple test-time scaling. *arXiv preprint arXiv:2501.19393*, 2025.

Dang Nguyen, Wenhan Yang, Rathul Anand, Yu Yang, and Baharan Mirzasoleiman. Mini-batch coresets for memory-efficient language model training on data mixtures. *arXiv preprint arXiv:2407.19580*, 2024.

OpenAI. Learning to reason with llms. <https://openai.com/index/learning-to-reason-with-llms/>, 2024.

Alec Radford, Jeffrey Wu, Rewon Child, David Luan, Dario Amodei, Ilya Sutskever, et al. Language models are unsupervised multitask learners. *OpenAI blog*, 1(8):9, 2019.

Charlie Snell, Jaehoon Lee, Kelvin Xu, and Aviral Kumar. Scaling llm test-time compute optimally can be more effective than scaling model parameters. *arXiv preprint arXiv:2408.03314*, 2024.

540 Jinyan Su, Jennifer Healey, Preslav Nakov, and Claire Cardie. Between underthinking and over-  
 541 thinking: An empirical study of reasoning length and correctness in llms. *arXiv preprint*  
 542 *arXiv:2505.00127*, 2025.

543 Yiyou Sun, Shawn Hu, Georgia Zhou, Ken Zheng, Hannaneh Hajishirzi, Nouha Dziri, and Dawn  
 544 Song. Omega: Can llms reason outside the box in math? evaluating exploratory, compositional,  
 545 and transformative generalization. *arXiv preprint arXiv:2506.18880*, 2025.

547 Ashish Vaswani, Noam Shazeer, Niki Parmar, Jakob Uszkoreit, Llion Jones, Aidan N Gomez, Łukasz  
 548 Kaiser, and Illia Polosukhin. Attention is all you need. *Advances in neural information processing*  
 549 *systems*, 30, 2017.

550 Roman Vershynin. Introduction to the non-asymptotic analysis of random matrices. In *Compressed*  
 551 *Sensing*, 2010.

553 Yuhang Wang, Youhe Jiang, Bin Cui, and Fangcheng Fu. Thinking short and right over thinking long:  
 554 Serving llm reasoning efficiently and accurately. *arXiv preprint arXiv:2505.13326*, 2025.

555 Sean Welleck, Amanda Bertsch, Matthew Finlayson, Hailey Schoelkopf, Alex Xie, Graham Neubig,  
 556 Ilia Kulikov, and Zaid Harchaoui. From decoding to meta-generation: Inference-time algorithms  
 557 for large language models. *arXiv preprint arXiv:2406.16838*, 2024.

559 Sang Michael Xie, Hieu Pham, Xuanyi Dong, Nan Du, Hanxiao Liu, Yifeng Lu, Percy S Liang,  
 560 Quoc V Le, Tengyu Ma, and Adams Wei Yu. Doremi: Optimizing data mixtures speeds up language  
 561 model pretraining. *Advances in Neural Information Processing Systems*, 36:69798–69818, 2023.

562 Edward Yeo, Yuxuan Tong, Morry Niu, Graham Neubig, and Xiang Yue. Demystifying long  
 563 chain-of-thought reasoning in llms. *arXiv preprint arXiv:2502.03373*, 2025.

565 Zhaojian Yu, Yinghao Wu, Yilun Zhao, Arman Cohan, and Xiao-Ping Zhang. Z1: Efficient test-time  
 566 scaling with code. *arXiv preprint arXiv:2504.00810*, 2025.

567 Ruiqi Zhang, Spencer Frei, and Peter L Bartlett. Trained transformers learn linear models in-context.  
 568 *Journal of Machine Learning Research*, 25(49):1–55, 2024.

569

570

571

572

573

574

575

576

577

578

579

580

581

582

583

584

585

586

587

588

589

590

591

592

593

594 **A PROOFS OF THEOREMS AND TECHNICAL LEMMAS**  
 595

596 **A.1 PROOF OF THEOREM 3.1**  
 597

598 **Lemma A.1** *Assume an initialization of the form*

$$600 \quad V(0) = \begin{bmatrix} 0 & 0 & 0 & 0 \\ 0 & 0 & 0 & 0 \\ V_{31}(0) & 0 & 0 & 0 \\ 0 & 0 & 0 & 0 \end{bmatrix}, \quad W(0) = \begin{bmatrix} 0 & 0 & cI & 0 \\ 0 & 0 & 0 & -c \\ 0 & 0 & 0 & 0 \\ 0 & 0 & 0 & 0 \end{bmatrix}.$$

604 *When the linear transformer is trained under gradient descent. Then  $V(t)$  and  $W(t)$  have the  
 605 following form:*

$$606 \quad V(t) = \begin{bmatrix} 0 & 0 & 0 & 0 \\ 0 & 0 & 0 & 0 \\ V_{31}(t) & 0 & 0 & 0 \\ 0 & 0 & 0 & 0 \end{bmatrix}, \quad W(t) = \begin{bmatrix} 0 & 0 & cI & 0 \\ 0 & 0 & 0 & W_{24}(t) \\ 0 & 0 & 0 & 0 \\ 0 & 0 & 0 & 0 \end{bmatrix}.$$

610 *with  $V_{31}(t) \in \mathbb{R}^{d \times d}$  and  $W_{24}(t) \in \mathbb{R}$ .*

612 Lemma A.1 is very similar to (Huang et al., 2025a, Lemma C.2). The difference is that here the  
 613 features covariance is non-identity, while we do not do CoT during training.

614 Given that several blocks of  $V(t)$  and  $W(t)$  remain zero across the gradient updates, we can reduce  
 615 the loss function in a simpler form. Define the shorthand  $\tilde{V}(t) := V_{31}(t) \in \mathbb{R}^{d \times d}$  and  $w(t) :=$   
 616  $W_{24}(t) \in \mathbb{R}$ . Invoking (A.3) we can rewrite the loss as follows:

$$617 \quad \begin{aligned} L(\theta(t)) &= \frac{1}{2} \mathbb{E} \left( \|f_{\text{LSA}}(E_\tau; \theta(t))_{[:, -1]} - (0_d, 0, w_\tau, 1)\|_{\ell_2}^2 \right) \\ 618 &= \frac{1}{2} \mathbb{E} \left( \left\| \begin{bmatrix} 0 \\ 0 \\ \hat{w}_0 \\ 1 \end{bmatrix} + \frac{1}{n} \begin{bmatrix} 0_d \\ 0 \\ V_{31}(t) X X^\top (c \hat{w}_0 + W_{24}(t) w_\tau) \\ 0 \end{bmatrix} - \begin{bmatrix} 0 \\ 0 \\ w_\tau \\ 1 \end{bmatrix} \right\|_{\ell_2}^2 \right) \\ 619 &= \frac{1}{2} \mathbb{E} \left( \|(\tilde{V}(t) w(t) \hat{\Lambda} - I) w_\tau\|_{\ell_2}^2 \right), \end{aligned} \tag{A.1}$$

620 with  $\hat{\Lambda} := X X^\top / n$ . As we see  $w(t)$  does not provide additional degree of freedom in minimizing  
 621 the loss since it appears as the term  $\tilde{V}(t) w(t)$ . This clarifies fixing  $w(t) = -c$  along the gradient  
 622 updates.

623 We then have

$$624 \quad L(\theta) = \frac{1}{2} \mathbb{E} \left[ \text{tr}(c^2 \tilde{V} \hat{\Lambda}^2 \tilde{V}^\top + I + 2c \tilde{V} \hat{\Lambda}) \right]$$

625 **Lemma A.2** *Let  $X \in \mathbb{R}^{d \times n}$  with columns drawn i.i.d from  $\mathcal{N}(0, \Lambda)$ . For any deterministic matrix  $A$   
 626 we have*

$$627 \quad \mathbb{E} \left( \frac{X X^\top}{n} A \frac{X X^\top}{n} \right) = \frac{n-1}{n} \Lambda A \Lambda + \frac{1}{n} (\Lambda (A + A^\top) \Lambda + \text{tr}(\Lambda A) \Lambda).$$

628 Using Lemma A.2 we have

$$629 \quad \mathbb{E}(\hat{\Lambda}^2) = \frac{n+1}{n} \Lambda^2 + \frac{1}{n} \text{tr}(\Lambda) \Lambda := \Gamma \Lambda.$$

630 Therefore,

$$631 \quad L(\theta) = \frac{c^2}{2} \text{tr}(\tilde{V} \Gamma \Lambda \tilde{V}^\top) + \frac{d}{2} + c \text{tr}(\tilde{V} \Lambda) \tag{A.2}$$

632 This is convex in  $\tilde{V}$  and so gradient descent with a fixed step size  $\eta \leq 1/L$  converges to its minimizer,  
 633 if  $\nabla_{\tilde{V}}^2 L \preceq L I$ . We have

$$634 \quad \nabla_{\tilde{V}}^2 L = c^2 \Gamma \Lambda,$$

648 so we can take  $L = c^2 \|\Gamma\Lambda\|_{\text{op}}$ . To find the minimizer of  $L(\theta)$ , we set its gradient to zero,  
649

$$650 \quad \frac{c^2}{2}(\Gamma\Lambda\tilde{V}^\top + \tilde{V}\Gamma\Lambda) + c\Lambda = 0,$$

652 which is a continuous-time Lyapunov equation (Note that  $\Gamma$  and  $\Lambda$  commute and both are symmetric).  
653 Hence, it has a unique solution given by  $\tilde{V} = -\frac{\Gamma^{-1}}{c}$ .  
654

655 As the final step, we show that  $V_*$  and  $W_*$  are also a global optimum for the population loss, even  
656 without making the specific structure imposed by gradient descent as described in Lemma A.1.  
657

658 We continue by computing the output of LSA, and recall that  $\hat{w}_0 = 0$ .  
659

$$\begin{aligned} 660 \quad & VE_\tau \cdot \frac{E_\tau^\top W E_\tau[:, -1]}{n} \\ 661 \quad & = \frac{1}{n} V \begin{bmatrix} X & 0 \\ y & 0 \\ 0_{d \times n} & 0 \\ 0_{1 \times n} & 1 \end{bmatrix} E_\tau^\top W \begin{bmatrix} 0 \\ 0 \\ 0 \\ 1 \end{bmatrix} \\ 662 \quad & = \frac{1}{n} V \begin{bmatrix} XX^\top & Xy^\top & 0 & 0 \\ yX^\top & yy^\top & 0 & 0 \\ 0_{d \times n} & 0_{d \times 1} & 0_{d \times 1} & 0_{d \times 1} \\ 0_{1 \times n} & 0_{1 \times n} & 0 & 1 \end{bmatrix}^\top \begin{bmatrix} W_{14} \\ W_{24} \\ W_{34} \\ W_{44} \end{bmatrix} \\ 663 \quad & = \frac{1}{n} V \begin{bmatrix} XX^\top W_{14} + Xy^\top W_{24} \\ yX^\top W_{14} + yy^\top W_{24} \\ 0 \\ W_{44}(t) \end{bmatrix} \end{aligned}$$

674 Therefore,

$$\begin{aligned} 675 \quad & f_{\text{LSA}}(E_\tau, \theta)[:, -1] - (0_a, 0, w_\tau, 1)^\top \\ 676 \quad & = \begin{bmatrix} 0 \\ 0 \\ 0 \\ 1 \end{bmatrix} + \frac{1}{n} V \begin{bmatrix} XX^\top W_{14} + Xy^\top W_{24} \\ yX^\top W_{14} + yy^\top W_{24} \\ 0 \\ W_{44} \end{bmatrix} - \begin{bmatrix} 0 \\ 0 \\ w_\tau \\ 1 \end{bmatrix} \\ 677 \quad & = \frac{1}{n} V \begin{bmatrix} XX^\top W_{14} + XX^\top w_\tau^\top W_{24} \\ w_\tau^\top XX^\top W_{14} + w_\tau^\top XX^\top w_\tau W_{24} \\ 0 \\ W_{44} \end{bmatrix} - \begin{bmatrix} 0 \\ 0 \\ w_\tau \\ 0 \end{bmatrix} \end{aligned}$$

685 The loss function is the expected squared norm of this object. To minimize it, we can make its first,  
686 second and last entries zero by setting the corresponding rows in  $V$  to zero. This gives us  
687

$$\begin{aligned} 688 \quad & L(\theta) \\ 689 \quad & \geq \frac{1}{2} \mathbb{E} \left( \left\| \frac{1}{n} (V_{31} + V_{32} w_\tau^\top) XX^\top (W_{14} + W_{24} w_\tau) - w_\tau + \frac{1}{n} V_{34} W_{44} \right\|_{\ell_2}^2 \right) \\ 690 \quad & = \frac{1}{2} \mathbb{E} \left( \left\| V_{31} \hat{\Lambda} W_{14} + \frac{1}{n} V_{34} W_{44} + (V_{31} \hat{\Lambda} W_{24} - I) w_\tau + V_{32} w_\tau^\top \hat{\Lambda} W_{14} + V_{32} w_\tau^\top \hat{\Lambda} W_{24} w_\tau \right\|_{\ell_2}^2 \right) \\ 691 \quad & \geq \frac{1}{2} \mathbb{E} \left( \left\| (V_{31} \hat{\Lambda} W_{24} - I) w_\tau + V_{32} w_\tau^\top \hat{\Lambda} W_{14} \right\|_{\ell_2}^2 \right) \\ 692 \quad & = \frac{1}{2} \mathbb{E} \left( \left\| (V_{31} W_{24} \hat{\Lambda} + V_{32} W_{14}^\top \hat{\Lambda} - I) w_\tau \right\|_{\ell_2}^2 \right), \end{aligned}$$

693 where the penultimate step holds since the cross term is an odd function of  $w_\tau$  and so its expectation  
694 is zero. The other eliminated term is squared and so non-negative. In the last step we used that  
695  $w_\tau^\top \hat{\Lambda} W_{14}$  is scalar and so can be replaced by its transpose. In addition  $W_{24}$  is also scalar and can  
696

702 commute with  $\hat{\Lambda}$ . now observe that  $V_{32}$  and  $W_{14}$  do not offer any flexibility in minimizing the loss  
 703 function as their effect can be absorbed in  $V_{31}W_{24}$ . Therefore, we can set them to zero. Hence,  
 704

$$705 \min_{V,W} L(\theta) \geq \min_{V_{31},W_{24}} \frac{1}{2} \mathbb{E} \left( \left\| (V_{31}W_{24}\hat{\Lambda} - I)w_\tau \right\|_{\ell_2}^2 \right).$$

706 Observe that the right-hand side is of the form (A.1) and hence its global optimum (reached by  
 707 gradient descent) serves as the global minimum of the loss.  
 708

709 **A.1.1 PROOF OF LEMMA A.1**

711 To prove this lemma, we prove that when the irrelevant blocks are 0, the gradients of the loss remain  
 712 zero on those blocks and they never update the corresponding parameter block.

713 We do induction on  $t$ . Suppose that the claim holds for  $t$ . We start by computing the output of LSA.  
 714

$$\begin{aligned} 715 \quad & VE_\tau \cdot \frac{E_\tau^\top W E_\tau[:, -1]}{n} \\ 716 \\ 717 \quad & = \frac{1}{n} \begin{bmatrix} 0 & 0 & 0 & 0 \\ 0 & 0 & 0 & 0 \\ V_{31}(t) & 0 & 0 & 0 \\ 0 & 0 & 0 & 0 \end{bmatrix} \begin{bmatrix} X & 0 \\ y & 0 \\ 0_{d \times n} & \hat{w}_0 \\ 0_{1 \times n} & 1 \end{bmatrix} E_\tau^\top W \begin{bmatrix} 0 \\ 0 \\ \hat{w}_0 \\ 1 \end{bmatrix} \\ 718 \\ 719 \quad & = \frac{1}{n} \begin{bmatrix} 0_{d \times n} & 0_d \\ 0_{1 \times n} & 0 \\ V_{31}(t)X & 0_d \\ 0_{1 \times n} & 0 \end{bmatrix} \begin{bmatrix} X & 0 \\ y & 0 \\ 0_{d \times n} & \hat{w}_0 \\ 0_{1 \times n} & 1 \end{bmatrix}^\top \begin{bmatrix} c\hat{w}_0 \\ W_{24}(t) \\ 0 \\ 0 \end{bmatrix} \\ 720 \\ 721 \quad & = \frac{1}{n} \begin{bmatrix} 0_{d \times n} & 0_d \\ 0_{1 \times n} & 0 \\ V_{31}(t)X & 0_d \\ 0_{1 \times n} & 0 \end{bmatrix} \begin{bmatrix} cX^\top \hat{w}_0 + W_{24}(t)y^\top \\ 0 \end{bmatrix} \\ 722 \\ 723 \quad & = \frac{1}{n} \begin{bmatrix} 0_d \\ 0 \\ V_{31}(t)XX^\top(c\hat{w}_0 + W_{24}(t)y^\top) \\ 0 \end{bmatrix}, \end{aligned} \tag{A.3}$$

724 where we used that  $y^\top = X^\top w_\tau^*$ . We proceed with calculating the derivatives of the loss:  
 725

$$\begin{aligned} 726 \quad & \nabla_V L(\theta(t)) = \frac{1}{2} \nabla_V \mathbb{E} \left( \left\| f_{\text{LSA}}(E_\tau; \theta(t))[:, -1] - (0_d, 0, w_\tau, 1) \right\|_{\ell_2}^2 \right) \\ 727 \\ 728 \quad & = \mathbb{E} \left[ (f_{\text{LSA}}(E_\tau; \theta(t))[:, -1] - (0_d, 0, w_\tau, 1)) E_\tau[:, -1]^\top W^\top \frac{E_\tau E_\tau^\top}{n} \right] \\ 729 \\ 730 \quad & = \mathbb{E} \left[ \left( VE_\tau \cdot \frac{E_\tau^\top W E_\tau[:, -1]}{n} - (0_d, 0, w_\tau - \hat{w}_0, 0) \right) E_\tau[:, -1]^\top W^\top \frac{E_\tau E_\tau^\top}{n} \right] \end{aligned} \tag{A.4}$$

731 We note that

$$\begin{aligned} 732 \quad & VE_\tau \cdot \frac{E_\tau^\top W E_\tau[:, -1]}{n} - (0_d, 0, w_\tau - \hat{w}_0, 0) \\ 733 \\ 734 \quad & = \frac{1}{n} \begin{bmatrix} 0_d \\ 0 \\ V_{31}(t)XX^\top(c\hat{w}_0 + W_{24}(t)y^\top) + n(\hat{w}_0 - w_\tau) \\ 0 \end{bmatrix}. \end{aligned} \tag{A.5}$$

735 In addition,

$$\begin{aligned} 736 \quad & E_\tau[:, -1]^\top W^\top \frac{E_\tau E_\tau^\top}{n} = \frac{1}{n} [c\hat{w}_0 \quad W_{24}(t) \quad 0 \quad 0] \begin{bmatrix} XX^\top & Xy^\top & 0 & 0 \\ yX^\top & yy^\top & 0 & 0 \\ 0 & 0 & \hat{w}_0 \hat{w}_0^\top & \hat{w}_0 \\ 0 & 0 & \hat{w}_0^\top & 1 \end{bmatrix} \\ 737 \\ 738 \quad & = \frac{1}{n} [c\hat{w}_0 XX^\top + W_{24}(t)yX^\top \quad c\hat{w}_0 Xy^\top + W_{24}(t)yy^\top \quad 0 \quad 0]. \end{aligned} \tag{A.6}$$

756 Plugging in from (A.5) and (A.6) into (A.4) we get the following structure for the gradient of the  
 757 loss:

$$759 \quad \nabla L(\theta(t)) = \begin{bmatrix} 0 & 0 & 0 & 0 \\ 0 & 0 & 0 & 0 \\ \nabla_{V_{31}} L(\theta(t)) & \nabla_{V_{32}} L(\theta(t)) & 0 & 0 \\ 0 & 0 & 0 & 0 \end{bmatrix}, \quad (A.7)$$

763 where

$$764 \quad \nabla_{V_{31}} L(\theta(t)) = \frac{1}{n^2} \mathbb{E} [(V_{31}(t)XX^\top(c\hat{w}_0 + W_{24}(t)w_\tau) + n(\hat{w}_0 - w_\tau))(c\hat{w}_0XX^\top + W_{24}(t)yy^\top)]$$

$$766 \quad \nabla_{V_{32}} L(\theta(t)) = \frac{1}{n^2} \mathbb{E} [(V_{31}(t)XX^\top(c\hat{w}_0 + W_{24}(t)w_\tau) + n(\hat{w}_0 - w_\tau))(c\hat{w}_0Xy^\top + W_{24}(t)yy^\top)]$$

768 Recall that we set  $\hat{w}_0 = 0$  by which we obtain

$$771 \quad \nabla_{V_{32}} L(\theta(t)) = \frac{1}{n^2} \mathbb{E} ((V_{31}(t)W_{24}(t)XX^\top - nI)w_\tau W_{24}(t)yy^\top)$$

$$772 \quad = \frac{W_{24}(t)}{n^2} \mathbb{E} ((V_{31}(t)W_{24}(t)XX^\top - nI)w_\tau w_\tau^\top XX^\top w_\tau) = 0$$

775 since it is an odd function of  $w_\tau \sim N(0, I)$ . (Note that the population loss is non-random, due to the  
 776 expectation in its definition. Since the initial  $V(0)$ ,  $W(0)$  are non-random, the trajectory  $V(t)$  and  
 777  $W(t)$  are non-random.)

778 We next proceed with calculating the gradient with respect to  $W$ . We have

$$780 \quad \nabla_W L(\theta(t))$$

$$781 \quad = \frac{1}{2} \nabla_W \mathbb{E} \left( \|f_{\text{LSA}}(E_\tau; \theta(t))_{[:, -1]} - (0_d, 0, w_\tau, 1)\|_{\ell_2}^2 \right)$$

$$783 \quad = \frac{1}{n} \mathbb{E} [E_\tau E_\tau^\top V^\top (f_{\text{LSA}}(E_\tau; \theta(t))_{[:, -1]} - (0_d, 0, w_\tau, 1)) E_\tau[:, -1]^\top]$$

$$785 \quad = \frac{1}{n} \mathbb{E} \left[ E_\tau E_\tau^\top V^\top \left( VE_\tau \cdot \frac{E_\tau^\top W E_\tau[:, -1]}{n} - (0_d, 0, w_\tau - \hat{w}_0, 0) \right) E_\tau[:, -1]^\top \right]$$

$$788 \quad = \frac{1}{n^2} \mathbb{E} \left( \begin{bmatrix} XX^\top V_{31}(t)^\top (V_{31}(t)XX^\top(c\hat{w}_0 + W_{24}(t)w_\tau) + n(\hat{w}_0 - w_\tau)) \\ yX^\top V_{31}(t)^\top (V_{31}(t)XX^\top(c\hat{w}_0 + W_{24}(t)w_\tau) + n(\hat{w}_0 - w_\tau)) \\ 0 \\ 0 \end{bmatrix} \begin{bmatrix} 0_d \\ 0 \\ \hat{w}_0 \\ 1 \end{bmatrix} \right),$$

792 where the last step follows from the following equation and simple algebraic calculation:

$$794 \quad E_\tau E_\tau^\top = \begin{bmatrix} XX^\top & Xy^\top & 0 & 0 \\ yX^\top & yy^\top & 0 & 0 \\ 0 & 0 & \hat{w}_0 \hat{w}_0^\top & \hat{w}_0 \\ 0 & 0 & \hat{w}_0^\top & 1 \end{bmatrix}, \quad E_\tau[:, -1]^\top = [0 \ 0 \ \hat{w}_0 \ 1],$$

$$798 \quad VE_\tau \cdot \frac{E_\tau^\top W E_\tau[:, -1]}{n} - (0_d, 0, w_\tau - \hat{w}_0, 0) = \begin{bmatrix} 0_d \\ 0 \\ V_{31}(t)XX^\top(c\hat{w}_0 + W_{24}(t)w_\tau) + n(\hat{w}_0 - w_\tau) \\ 0 \end{bmatrix}$$

802 Recalling that  $\hat{w}_0 = 0$  we simplify  $\nabla_W L$  as follows:

$$804 \quad \nabla_W L(\theta(t)) = \frac{1}{n^2} \mathbb{E} \left( \begin{bmatrix} XX^\top V_{31}(t)^\top (V_{31}(t)W_{24}(t)XX^\top - nI)w_\tau \\ yX^\top V_{31}(t)^\top (V_{31}(t)W_{24}(t)XX^\top - nI)w_\tau \\ 0 \\ 0 \end{bmatrix} \begin{bmatrix} 0 \\ 0 \\ 0 \\ 1 \end{bmatrix} \right). \quad (A.8)$$

809 We have  $\mathbb{E}[XX^\top V_{31}(t)^\top (V_{31}(t)W_{24}(t)XX^\top + nI)w_\tau] = 0$ , since  $V_{31}(t)$ ,  $W_{24}(t)$  are non-random  
 810 and  $w_\tau$  is zero mean and independent of  $X$ . Hence,  $\nabla_{W_{24}} L$  is the only non-zero block.

## A.1.2 PROOF OF LEMMA A.2

$$\frac{1}{n^2} \mathbb{E} [XX^\top AXX^\top] = \frac{1}{n^2} \sum_{i,j} \mathbb{E} [x_i x_i^\top A x_j x_j^\top]$$

There are  $n(n-1)$  terms where  $i \neq j$  and  $n$  terms with  $i = j$ . Since  $x_i$  and  $x_j$  are i.i.d., let  $x$  denote either of them. Thus,

$$\frac{1}{n^2} \mathbb{E} [XX^\top AXX^\top] = \frac{1}{n^2} (n(n-1) \mathbb{E}[xx^\top] A \mathbb{E}[xx^\top] + n \mathbb{E}[xx^\top Axx^\top])$$

The first term is the second moments. For the second term we use Isserlis's theorem, by which we have

$$\begin{aligned} (\mathbb{E}[xx^\top Axx^\top])_{ij} &= \sum_{k,l} \mathbb{E}[x_i x_k A_{kl} x_l x_j] \\ &= \sum_{k,l} A_{kl} (\mathbb{E}[x_i x_k] \mathbb{E}[x_l x_j] + \mathbb{E}[x_i x_l] \mathbb{E}[x_k x_j] + \mathbb{E}[x_i x_j] \mathbb{E}[x_l x_k]) \end{aligned}$$

Assuming  $\mathbb{E}[xx^\top] = \Lambda$ , we get

$$\mathbb{E}[xx^\top Axx^\top] = \Lambda(A + A^\top)\Lambda + \Lambda \operatorname{Tr}(A\Lambda).$$

Therefore we obtain

$$\frac{1}{n^2} \mathbb{E} [XX^\top AXX^\top] = \frac{n-1}{n^2} \Lambda A \Lambda + \frac{1}{n} (\Lambda(A + A^\top)\Lambda + \Lambda \operatorname{Tr}(A\Lambda)).$$

## A.2 PROOF OF PROPOSITION 3.2

Recall  $V_*$  and  $W_*$  given by (3.6), as the estimated blocks of the transformer after training. We next rewrite the updates for  $w_i$  in a more explicit form:

$$\begin{aligned} f_{\text{LSA}}(E_i, \theta^*)_{[:, -1]} &= \begin{bmatrix} 0_d \\ 0 \\ w_i \\ 1 \end{bmatrix} + V E_i \cdot \frac{E_i^\top W E_i_{[:, -1]}}{m} \\ &= \begin{bmatrix} 0_d \\ 0 \\ w_i \\ 1 \end{bmatrix} + \frac{1}{m} V E_i E_i^\top \begin{bmatrix} cw_i \\ -c \\ 0 \\ 0 \end{bmatrix} \\ &= \begin{bmatrix} 0_d \\ 0 \\ w_i \\ 1 \end{bmatrix} + \frac{1}{m} V \begin{bmatrix} XX^\top & Xy^\top \\ yX^\top & yy^\top \\ 0_{d \times d} & 0_{m \times m} \\ 0 & 0 \end{bmatrix} \begin{bmatrix} cw_i \\ -c \\ 0 \\ 0 \end{bmatrix} \\ &= \begin{bmatrix} 0_d \\ 0 \\ w_i \\ 1 \end{bmatrix} + \frac{1}{m} \begin{bmatrix} 0 & 0 \\ 0 & 0 \\ V_{31} XX^\top & V_{31} Xy^\top \\ 0 & 0 \end{bmatrix} \begin{bmatrix} cw_i \\ -c \\ 0 \\ 0 \end{bmatrix} \end{aligned}$$

Recalling that  $V_{31} = \Gamma^{-1}/c$  we obtain

$$\begin{aligned} w_{i+1} &= w_i - \frac{1}{m} \Gamma^{-1} X_{\text{test}} X_{\text{test}}^\top w_i - \frac{1}{m} \Gamma^{-1} X_{\text{test}} y_{\text{test}}^\top \\ &= w_i - \frac{1}{m} \Gamma^{-1} X_{\text{test}} X_{\text{test}}^\top (w_i - w_{\text{test}}). \end{aligned}$$

Rearranging the terms,  $w_{i+1} - w_{\text{test}} = (I - \frac{1}{m} \Gamma^{-1} X_{\text{test}} X_{\text{test}}^\top)(w_i - w_{\text{test}})$  which results in

$$\begin{aligned} w_{k+1} &= w_{\text{test}} + (I - \frac{1}{m} \Gamma^{-1} X_{\text{test}} X_{\text{test}}^\top)^k (w_0 - w_{\text{test}}) \\ &= (I - (I - \frac{1}{m} \Gamma^{-1} X_{\text{test}} X_{\text{test}}^\top)^k) w_{\text{test}}, \end{aligned} \tag{A.9}$$

which completes the proof.

864 A.3 PROOF OF THEOREM 3.3  
865866 Define the shorthand  $\hat{\Lambda} = X_{\text{test}} X_{\text{test}}^\top / m$ . We have  
867

868 
$$\mathbb{E}(\|\hat{w} - w_{\text{test}}\|_{\ell_2}^2) = \mathbb{E}(\left\|(I - \Gamma^{-1}\hat{\Lambda})w_{\text{test}}\right\|_{\ell_2}^2) = w_{\text{test}}^\top \mathbb{E}((I - \hat{\Lambda}\Gamma^{-1})(I - \Gamma^{-1}\hat{\Lambda}))w_{\text{test}}$$
  
869  
870 
$$= w_{\text{test}}^\top (I - \Gamma^{-1}\Lambda - \Lambda\Gamma^{-1} + \mathbb{E}(\hat{\Lambda}\Gamma^{-2}\hat{\Lambda}))w_{\text{test}}$$
  
871

872 Using Lemma A.2 we have  
873

874 
$$\mathbb{E}(\hat{\Lambda}\Gamma^{-2}\hat{\Lambda}) = \frac{m-1}{m}\Lambda\Gamma^{-2}\Lambda + \frac{1}{m}(2\Lambda\Gamma^{-2}\Lambda + \text{tr}(\Lambda\Gamma^{-2})\Lambda)$$
  
875  
876 
$$= \frac{m+1}{m}\Lambda\Gamma^{-2}\Lambda + \frac{1}{m}\text{tr}(\Lambda\Gamma^{-2})\Lambda.$$
  
877

878 Using that  $\Gamma^{-1}$  and  $\Lambda$  commute and both are symmetric we obtain  
879

880 
$$\mathbb{E}(\|\hat{w} - w_{\text{test}}\|_{\ell_2}^2) = w_{\text{test}}^\top (I - 2\Gamma^{-1}\Lambda + \frac{m+1}{m}\Gamma^{-2}\Lambda^2 + \frac{1}{m}\text{tr}(\Lambda\Gamma^{-2})\Lambda)w_{\text{test}}$$
  
881  
882 
$$= w_{\text{test}}^\top (I - \Gamma^{-1}\Lambda)^2 w_{\text{test}} + \frac{1}{m}w_{\text{test}}^\top (\Gamma^{-2}\Lambda^2 + \text{tr}(\Lambda\Gamma^{-2})\Lambda)w_{\text{test}}$$
  
883

884 Using the definition  $\Gamma = (1 + \frac{1}{n})\Lambda + \frac{1}{n}\text{tr}(\Lambda)I$ , it is easy to see that  
885

886 
$$0 \preceq I - \Gamma^{-1}\Lambda \preceq \frac{1}{n}(I + \text{tr}(\Lambda)\Lambda^{-1})$$
  
887

888 Also since  $\Gamma^{-1} \preceq \Lambda^{-1}$ , we have  
889

890 
$$\Gamma^{-2}\Lambda^2 + \text{tr}(\Lambda\Gamma^{-2})\Lambda \preceq I + \text{tr}(\Lambda^{-1})\Lambda$$
  
891

892 Combining the last two equations, we have  
893

894 
$$\mathbb{E}_{X_{\text{test}}}(\|\hat{w} - w_{\text{test}}\|_{\ell_2}^2) \leq w_{\text{test}}^\top \left( \frac{1}{n^2}(I + \text{tr}(\Lambda)\Lambda^{-1})^2 + \frac{1}{m}(I + \text{tr}(\Lambda^{-1})\Lambda) \right) w_{\text{test}}$$
  
895

896 Taking another expectation with respect to  $w_{\text{test}} \sim \mathcal{N}(0, I)$  we get  
897

898 
$$\mathbb{E}(\|\hat{w} - w_{\text{test}}\|_{\ell_2}^2) \leq \frac{1}{n^2}(d + \text{tr}(\Lambda)^2\text{tr}(\Lambda^{-2}) + 2\text{tr}(\Lambda)\text{tr}(\Lambda^{-1})) + \frac{1}{m}(d + \text{tr}(\Lambda^{-1})\text{tr}(\Lambda))$$
  
899

900 The claim follows by noting  
901

902 
$$\text{tr}(\Lambda)\text{tr}(\Lambda^{-1}) \leq d \frac{\text{tr}(\Lambda)}{\lambda_{\min}},$$
  
903  
904 
$$\text{tr}(\Lambda)^2\text{tr}(\Lambda^{-2}) \leq d \left( \frac{\text{tr}(\Lambda)}{\lambda_{\min}} \right)^2,$$
  
905

906 where  $\lambda_{\min}$  is the minimum eigenvalue of  $\Lambda$ .  
907908 A.4 PROOF OF THEOREM 3.4  
909910 We define  $\hat{\Lambda} := \frac{1}{m} \sum_{i=1}^k x_i x_i^\top$ . After  $k$  steps generation, we have  $w_{k+1} = (I - (I - \Gamma^{-1}\hat{\Lambda})^k)w_{\text{test}}$   
911 and so  
912

913 
$$\mathbb{E}(\|w_{k+1} - w_{\text{test}}\|_{\ell_2}^2) = \mathbb{E}(\left\|(I - \Gamma^{-1}\hat{\Lambda})^k w_{\text{test}}\right\|_{\ell_2}^2) = \mathbb{E} \text{tr}((I - \hat{\Lambda}\Gamma^{-1})^k (I - \Gamma^{-1}\hat{\Lambda})^k). \quad (\text{A.10})$$
  
914

915 Note that  $\Gamma^{-1}$  and  $\Lambda$  commute and both are symmetric. Therefore  $\Gamma^{-1}\Lambda$  is also symmetric. We denote  
916 by  $\sigma_i$  the eigenvalues of  $I - \Gamma^{-1}\Lambda$ . The matrix  $I - \Gamma^{-1}\hat{\Lambda}$  however is not symmetric. We denote by  
917  $\hat{\sigma}_i$  the eigenvalues of  $I - \Gamma^{-1}\hat{\Lambda}$ . By Weyl's inequality, we have  $|\sigma_i - \hat{\sigma}_i| \leq \left\| \Gamma^{-1}(\Lambda - \hat{\Lambda}) \right\|_{\text{op}} := \delta$ .  
918

918 We then have  
 919

$$\begin{aligned}
 \hat{\sigma}_i^{2k} &\leq (\sigma_i + \delta)^{2k} \\
 &= \sigma_i^{2k} \left(1 + \frac{\delta}{\sigma_i}\right)^{2k} \\
 &= \sigma_i^{2k} \left(1 + \sum_{j=1}^{2k} \binom{2k}{j} \left(\frac{\delta}{\sigma_i}\right)^j\right) \\
 &\leq \sigma_i^{2k} \left(1 + \sum_{j=1}^{2k} (2k)^j \left(\frac{\delta}{\sigma_i}\right)^j\right)
 \end{aligned} \tag{A.11}$$

930 Define  $\tilde{\Delta}_i := \sum_{j=1}^{2k} \left(\frac{2k\delta}{\sigma_i}\right)^j$ . We next proceed by bounding  $\mathbb{E}(\tilde{\Delta}_i)$ . Observe that  $\hat{\Lambda} =$   
 931  $\frac{1}{m} \sum_{i \in [m]} x_i x_i^\top$ , with  $x_i \sim \mathcal{N}(0, \Lambda)$ . Using concentration bounds on random matrices with in-  
 932 dependent sub-gaussian rows (See e.g. (Vershynin, 2010, Eq. 5.26)), we get that with probability at  
 933 least  $1 - 2e^{-ct^2}$ ,  
 934

$$\|\Lambda - \hat{\Lambda}\|_{\text{op}} \leq \max(\varepsilon, \varepsilon^2) \|\Lambda\|_{\text{op}}, \quad \varepsilon = C \sqrt{\frac{d}{m}} + \frac{t}{\sqrt{m}}.$$

935 Since  $\Lambda$  and so  $\Gamma$  have bounded eigenvalues, by adjusting the constants  $c, C$  (absorbing  $\|\Lambda\|_{\text{op}}$  and  
 936  $\|\Gamma^{-1}\|_{\text{op}}$  into these constants), we also have that with probability at least  $1 - 2e^{-ct^2}$ ,  
 937

$$\delta := \|\Gamma^{-1}(\Lambda - \hat{\Lambda})\|_{\text{op}} \leq \max(\varepsilon, \varepsilon^2), \quad \varepsilon = C \sqrt{\frac{d}{m}} + \frac{t}{\sqrt{m}}. \tag{A.12}$$

938 We define the probabilistic event  $\mathcal{E} := \{\tilde{\Delta}_i \leq Ck^2 \sqrt{d/m}\}$ . Obviously,  $\mathbb{E}(\tilde{\Delta}_i \mathbf{1}_{\mathcal{E}}) \leq Ck^2 \sqrt{d/m}$ .  
 939 We also have  $\mathbb{E}(\tilde{\Delta}_i \mathbf{1}_{\mathcal{E}^c}) = \int_{Ck^2 \sqrt{d/m}}^{\infty} \mathbb{P}(\tilde{\Delta}_i \geq s) ds$ . Note that by definition of  $\tilde{\Delta}_i$ , we have  
 940

$$\tilde{\Delta}_i = \sum_{j=1}^{2k} \left(\frac{2k\delta}{\sigma_i}\right)^j \leq 2k \max\left(2k\delta/\sigma_i, (2k\delta/\sigma_i)^{2k}\right) \leq C'k \max(k\delta, (k\delta)^{2k}).$$

941 Note that since eigenvalues of  $\Lambda$  are upper and lower bounded by constants, so are  $\sigma_i$ 's. Therefore,  
 942 we can work with one constant  $C'$  that works for all  $i \in [d]$ .  
 943

944 By virtue of the above bound, if  $\tilde{\Delta}_i \geq s$  we have  $\delta \geq \min\left(\frac{s}{k^2}, \left(\frac{s}{k^{2k+1}}\right)^{\frac{1}{2k}}\right) \geq \frac{1}{k^2} \min(s, s^{\frac{1}{2k}})$ . We  
 945 next choose  $t$  such that for  $\varepsilon = C \sqrt{\frac{d}{m}} + \frac{t}{\sqrt{m}}$  we have  $\max(\varepsilon, \varepsilon^2) \leq \frac{1}{k^2} \min(s, s^{\frac{1}{2k}})$ , so that we can  
 946 apply the tail bound (A.12).  
 947

948 In addition, for  $s \geq Ck^2 \sqrt{d/m}$  we have  $\frac{1}{k^2} \min(s, s^{\frac{1}{2k}}) \geq C \sqrt{d/m}$ , and so it suffices to have  
 949  $\max\left(\frac{t}{\sqrt{m}}, \frac{t^2}{m}\right) \leq \frac{1}{k^2} \min(s, s^{\frac{1}{2k}})$ . Therefore, we can set  $t = \min\left(\frac{\sqrt{m}}{k^2} s, \frac{\sqrt{m}}{k^2} s^{\frac{1}{2k}}, \frac{\sqrt{m}}{k} \sqrt{s}, \frac{\sqrt{m}}{k} s^{\frac{1}{4k}}\right)$ .  
 950

$$\begin{aligned}
 \mathbb{E}(\tilde{\Delta}_i \mathbf{1}_{\mathcal{E}^c}) &= \int_{Ck^2 \sqrt{d/m}}^{\infty} \mathbb{P}(\tilde{\Delta}_i \geq s) ds \\
 &\leq \int_{Ck^2 \sqrt{d/m}}^{\infty} \mathbb{P}\left(\delta \geq \frac{1}{k^2} \min(s, s^{\frac{1}{2k}})\right) \\
 &\leq \int_{Ck^2 \sqrt{d/m}}^{\infty} 2 \exp(-ct^2) ds
 \end{aligned}$$

951 By considering each of the four terms in the minimum operator defining  $t$ , and following algebraic  
 952 manipulation, it can be seen that the right-hand side above is  $O(k^2 \sqrt{d/m})$  and hence,  
 953

$$\mathbb{E}(\tilde{\Delta}_i) = \mathbb{E}(\tilde{\Delta}_i \mathbf{1}_{\mathcal{E}}) + \mathbb{E}(\tilde{\Delta}_i \mathbf{1}_{\mathcal{E}^c}) \leq C(k \sqrt{d/m}), \tag{A.13}$$

972 for a constant  $C > 0$  and for all  $i \in [d]$ . Combining (A.10) and (A.14) and the bound  $\tilde{\Delta}_i$ , we obtain  
 973

$$\begin{aligned}
 974 \quad \mathbb{E}(\|w_{k+1} - w_{\text{test}}\|_{\ell_2}^2) &\leq \mathbb{E}[\|(I - \hat{\Lambda}\Gamma^{-1})^k\|_F^2] \\
 975 &\stackrel{(a)}{\leq} \mathbb{E}(\sum_{i=1}^d \hat{\sigma}_i^{2k}) \\
 976 &\stackrel{(b)}{\leq} \sum_{i=1}^d \sigma_i^{2k}(1 + \mathbb{E}(\tilde{\Delta}_i)) \\
 977 &\stackrel{(c)}{\leq} \sum_{i=1}^d \sigma_i^{2k}(1 + Ck\sqrt{\frac{d}{m}}) \\
 978 &= \text{tr}((I - \Gamma^{-1}\Lambda)^{2k})(1 + Ck\sqrt{\frac{d}{m}}),
 \end{aligned}$$

986 where (b) follows from (A.11) and (c) follows from (A.13). In addition, step (a) follows from the  
 987 following lemma from Horn & Johnson (1994).

988 **Lemma A.3** ((Horn & Johnson, 1994, Eq.(3.3.39))) *Let  $A$  be a given  $d$  by  $d$  matrix and let  $m$  be a  
 989 given positive integer. For all  $p > 0$  we have*

$$\sum_{i=1}^q \sigma_i(A^m)^p \leq \sum_{i=1}^q \sigma_i(A)^{mp}, \quad \text{for } q = 1, \dots, d,$$

994 where for a matrix  $B$ ,  $\sigma_i(B)$  denotes the singular values of  $B$ .

995 Step (a) follows by using the above lemma for  $A = (I - \hat{\Lambda}\Gamma^{-1})^k$ ,  $m = k$ ,  $p = 2$ ,  $q = d$ . This  
 996 completes the proof.

## 998 A.5 PROOF OF COROLLARY 3.5

1000 Recalling the definition of  $\Gamma$  given by (3.5), we have

$$\begin{aligned}
 1001 \quad I - \Gamma^{-1}\Lambda &= I - \left[(1 + \frac{1}{n})\Lambda + \frac{1}{n}\text{tr}(\Lambda)I\right]^{-1}\Lambda \\
 1002 &= [(n + 1)\Lambda + \text{tr}(\Lambda)I]^{-1}(\Lambda + \text{tr}(\Lambda)I) \\
 1003 &\leq \frac{\lambda_{\min} + \text{tr}(\Lambda)}{(n + 1)\lambda_{\min} + \text{tr}(\Lambda)}I \\
 1004 &= \frac{1 + \text{Hard}(\Lambda)}{n + 1 + \text{Hard}(\Lambda)}I \\
 1005 &= \left(1 + \frac{n}{1 + \text{Hard}(\Lambda)}\right)^{-1}I.
 \end{aligned}$$

1012 Therefore,

$$\text{tr}((I - \Gamma^{-1}\Lambda)^{2k}) \leq d \left(1 + \frac{n}{1 + \text{Hard}(\Lambda)}\right)^{-2k},$$

1015 which completes the proof by invoking the result of Theorem 3.4.

## 1017 A.6 PROOF OF THEOREM 4.1

1019 The proof follows a long the same lines as in Theorem 3.1. Under the multi-task setting, each feature  
 1020  $x$  is now coming from a mixture of normal distributions. The main modification needed in the proof  
 1021 is on statement of Lemma A.2, which is extended as follows.

1022 **Lemma A.4** *Let  $X \in \mathbb{R}^{d \times n}$  with columns drawn i.i.d from a Gaussian mixture distribution, with  
 1023 probability  $\pi_\ell$  from  $\mathcal{N}(0, \Lambda_\ell)$ . Then, for any deterministic matrix  $A$  we have*

$$\mathbb{E}\left(\frac{XX^\top}{n} A \frac{XX^\top}{n}\right) = \frac{n-1}{n}(\sum_\ell \Lambda_\ell \pi_\ell) A (\sum_\ell \Lambda_\ell \pi_\ell) + \frac{1}{n} \sum_\ell (\Lambda_\ell (A + A^\top) \Lambda_\ell + \Lambda_\ell \text{tr}(A \Lambda_\ell)) \pi_\ell.$$

1026 Using Lemma A.4, we have  
 1027

1028 
$$S := \mathbb{E} \left( \frac{XX^\top}{n} \frac{XX^\top}{n} \right) = \frac{n-1}{n} \left( \sum_\ell \Lambda_\ell \pi_\ell \right)^2 + \frac{1}{n} \sum_\ell (2\Lambda_\ell^2 + \Lambda_\ell \text{tr}(\Lambda_\ell)) \pi_\ell.$$
  
 1029  
 1030

1031 Continuing from (A.2), we have  
 1032

1033 
$$L(\theta) = \frac{c^2}{2} \text{tr} \left( \tilde{V} S \tilde{V}^\top \right) + \frac{d}{2} + c \text{tr} \left( \tilde{V} \left( \sum_\ell \Lambda_\ell \pi_\ell \right) \right)$$
  
 1034  
 1035

1036 Setting the derivative to zero, we obtain  
 1037

1038 
$$\nabla L(\theta) = \frac{c^2}{2} (\tilde{V} (S + S^\top)) + c \sum_\ell \Lambda_\ell \pi_\ell.$$
  
 1039  
 1040

1041 Solving this equation, using that  $S$  is symmetric, we have  
 1042

1043 
$$\tilde{V} = -\frac{1}{c} \left( \sum_\ell \Lambda_\ell \pi_\ell \right) S^{-1} = \frac{1}{c} \Gamma^{-1},$$
  
 1044  
 1045

1046 where the last step follows from the definition of  $\Gamma$ .  
 1047

### 1049 A.7 PROOF OF PROPOSITION 4.2

1050 The proof is similar to the proof of Theorem 3.4. Recall  $\widehat{\Sigma} := \frac{1}{m} X_{\text{test}} X_{\text{test}}^\top = \frac{1}{m} \sum_{i=1}^k x_i x_i^\top$ ,  
 1051 the empirical covariance of the features in the test prompt. A major difference with the proof of  
 1052 Theorem 3.4, here we have to work with  $\Gamma^{-1} \widehat{\Sigma}$  and  $\Gamma^{-1} \Sigma$ , neither of which are symmetric. To relate  
 1053 the trace of their powers to their singular values, we do a symmetrization step. We write  
 1054

1055 
$$\begin{aligned} & (I - \Gamma^{-1} \widehat{\Sigma})^k \\ &= (I - \Gamma^{-1} \widehat{\Sigma})(I - \Gamma^{-1} \widehat{\Sigma}) \dots (I - \Gamma^{-1} \widehat{\Sigma}) \\ &= \Gamma^{-1/2} \Gamma^{1/2} (I - \Gamma^{-1} \widehat{\Sigma}) \Gamma^{-1/2} \Gamma^{1/2} (I - \Gamma^{-1} \widehat{\Sigma}) \Gamma^{-1/2} \Gamma^{1/2} \dots \Gamma^{-1/2} \Gamma^{1/2} (I - \Gamma^{-1} \widehat{\Sigma}) \\ &= \Gamma^{-1/2} (I - \Gamma^{-1/2} \widehat{\Sigma} \Gamma^{-1/2}) (I - \Gamma^{-1/2} \widehat{\Sigma} \Gamma^{-1/2}) \dots (I - \Gamma^{-1/2} \widehat{\Sigma} \Gamma^{-1/2}) \Gamma^{1/2} \\ &= \Gamma^{-1/2} (I - \Gamma^{-1/2} \widehat{\Sigma} \Gamma^{-1/2})^k \Gamma^{1/2}. \end{aligned}$$
  
 1056  
 1057

1058 Hence,  
 1059

1060 
$$\begin{aligned} \text{tr}((I - \widehat{\Sigma} \Gamma^{-1})^k (I - \Gamma^{-1} \widehat{\Sigma})^k) &= \text{tr}(\Gamma^{1/2} (I - \Gamma^{-1/2} \widehat{\Sigma} \Gamma^{-1/2})^k \Gamma^{-1} (I - \Gamma^{-1/2} \widehat{\Sigma} \Gamma^{-1/2})^k \Gamma^{1/2}) \\ &= \text{tr}((I - \Gamma^{-1/2} \widehat{\Sigma} \Gamma^{-1/2})^k \Gamma^{-1} (I - \Gamma^{-1/2} \widehat{\Sigma} \Gamma^{-1/2})^k \Gamma) \\ &\leq \text{tr}((I - \Gamma^{-1/2} \widehat{\Sigma} \Gamma^{-1/2})^k \Gamma^{-1} (I - \Gamma^{-1/2} \widehat{\Sigma} \Gamma^{-1/2})^k) \text{tr}(\Gamma) \\ &= \text{tr}((I - \Gamma^{-1/2} \widehat{\Sigma} \Gamma^{-1/2})^k \Gamma^{-1} (I - \Gamma^{-1/2} \widehat{\Sigma} \Gamma^{-1/2})^k) \text{tr}(\Gamma) \\ &= \text{tr}((I - \Gamma^{-1/2} \widehat{\Sigma} \Gamma^{-1/2})^{2k} \Gamma^{-1}) \text{tr}(\Gamma) \\ &\leq \text{tr}((I - \Gamma^{-1/2} \widehat{\Sigma} \Gamma^{-1/2})^{2k}) \text{tr}(\Gamma^{-1}) \text{tr}(\Gamma). \end{aligned} \tag{A.14}$$
  
 1061  
 1062  
 1063

1064 In the equalities above we used the identity  $\text{tr}(AB) = \text{tr}(BA)$ . The inequalities follows from the  
 1065 fact that for positive semidefinite matrices  $A, B$  we have  $\text{tr}(AB) \leq \text{tr}(A)\text{tr}(B)$ .  
 1066

1067 We next denote by  $\hat{\sigma}_i$  the eigenvalues of  $I - \Gamma^{-1/2} \widehat{\Sigma} \Gamma^{-1/2}$ , and by  $\sigma_i$  the eigenvalues of  $I -$   
 1068  $\Gamma^{-1/2} \Sigma \Gamma^{-1/2}$ . Similar to the proof of Theorem 3.4, we have  $\hat{\sigma}_i^{2k} \leq \sigma_i^{2k} (1 + \hat{\Delta}_i)$  with  $\mathbb{E}(\hat{\Delta}_i) \leq$   
 1069  $Ck\sqrt{d/m}$  for all  $i \in [d]$ .  
 1070  
 1071

1080 By continuing from (A.14), we get  
 1081

$$\begin{aligned}
 1082 \mathbb{E}[\text{tr}((I - \widehat{\Sigma}\Gamma^{-1})^k(I - \Gamma^{-1}\widehat{\Sigma})^k)] &\leq \text{tr}(\Gamma^{-1})\text{tr}(\Gamma)\mathbb{E}[\text{tr}((I - \Gamma^{-1/2}\widehat{\Sigma}\Gamma^{-1/2})^{2k})] \\
 1083 &\leq \text{tr}(\Gamma^{-1})\text{tr}(\Gamma)\mathbb{E}[\sum_{i=1}^d \widehat{\sigma}_i^{2k}] \\
 1084 &\leq \text{tr}(\Gamma^{-1})\text{tr}(\Gamma)\sum_{i=1}^d \sigma_i^{2k}(1 + \mathbb{E}(\tilde{\Delta}_i)) \\
 1085 &\leq \text{tr}(\Gamma^{-1})\text{tr}(\Gamma)\sum_{i=1}^d \sigma_i^{2k}(1 + Ck\sqrt{d/m}) \\
 1086 &= \text{tr}(\Gamma^{-1})\text{tr}(\Gamma)\text{tr}((I - \Gamma^{-1/2}\Sigma\Gamma^{-1/2})^{2k})(1 + o(1)),
 \end{aligned}$$

1094 where in the last step we used that  $k\sqrt{d/m} = o(1)$  by our assumption. This concludes the proof.  
 1095

### 1096 A.8 PROOF OF PROPOSITION 4.3

1097 The proof follows from the Markov inequality. Define a discrete random variable  $X$  which takes  
 1098 values  $\sigma_{\min}(\Lambda_\ell)$  with probability  $\pi_\ell$ , for  $\ell \in [T]$ . We then have  
 1099

$$\mathbb{P}(X \leq 2(\varepsilon + \sigma_{\min}(\Sigma))) = \sum_{\ell \in [T]} \pi_\ell \mathbf{1}_{(\sigma_{\min}(\Lambda_\ell) \leq 2(\varepsilon + \sigma_{\min}(\Sigma)))} = \sum_{\ell \in D} \pi_\ell.$$

1100 In addition,

$$\mathbb{E}[X] = \sum \pi_\ell \sigma_{\min}(\Lambda_\ell) \leq \sigma_{\min}(\sum \pi_\ell \Lambda_\ell) = \sigma_{\min}(\tilde{\Gamma}),$$

1101 by using the convexity of minimum eigenvalue and Jensen's inequality.  
 1102

1103 Recalling  $\Gamma$  from (4.1), we have

$$\Gamma \succeq \frac{n-1}{n} \sum_{\ell \in [T]} \Lambda_\ell \pi_\ell = \frac{n-1}{n} \tilde{\Gamma} \succeq \frac{1}{2} \tilde{\Gamma},$$

1104 for  $n \geq 2$ . Combining the above two equations, we obtain  
 1105

$$\mathbb{E}[X] \leq 2\sigma_{\min}(\Gamma) \leq 2(\sigma_{\min}(\Sigma) + \varepsilon).$$

1106 Therefore,

$$\begin{aligned}
 1107 \sum_{\ell \in D} \pi_\ell &= \mathbb{P}(X \leq 4(\varepsilon + \sigma_{\min}(\Sigma))) \\
 1108 &= 1 - \mathbb{P}(X > 4(\varepsilon + \sigma_{\min}(\Sigma))) \\
 1109 &\geq 1 - \frac{\mathbb{E}[X]}{4(\varepsilon + \sigma_{\min}(\Sigma))} \\
 1110 &\geq 1 - \frac{1}{2} = \frac{1}{2},
 \end{aligned}$$

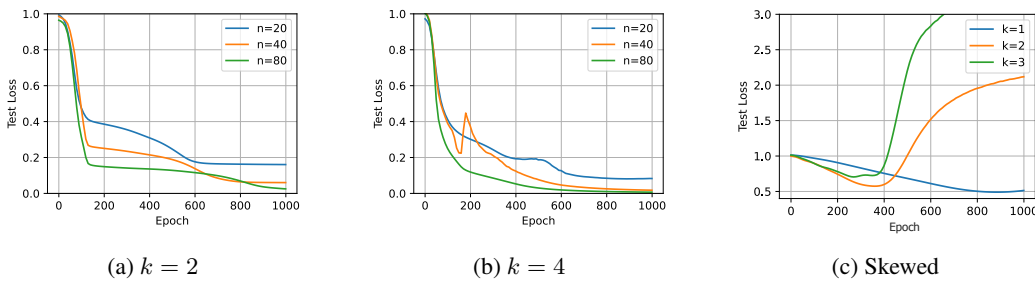
1111 where we used Markov's inequality in the third step.  
 1112

## 1113 B ADDITIONAL EXPERIMENTS

1114 We report additional experiments on a transformer with a single linear self-attention, when starting  
 1115 training from random initialization and performing CoT with length  $k$  during training. Similar to  
 1116 the main paper, the data distribution follows our in-context weight prediction task in Sec. 3.1, where  
 1117  $x_{\tau,i} \sim \mathcal{N}(0, \Lambda)$ ,  $w_\tau \sim \mathcal{N}(0, I_d)$ . We choose the token dimensions  $d = 10$ . During inference, we  
 1118 let model to output  $k$  steps before outputting the final predicted weight vector. At each step  $i$  we  
 1119 concatenate the embedding with  $[0_d, \hat{w}_i, 1]$  as in Eq. 3.1 and input the concatenated embedding  
 1120 matrix to the model. The predicted  $w_k$  will be outputted after  $k$  steps of CoT.  
 1121

1134 Fig. 4a, 4b show the test loss during training for  $k = 2, 4$ . For each  $k$ , we train the model with  
 1135  $n = 20, 40, 80$ . The training and test data are generated from  $x_{\tau,i} \sim \mathcal{N}(0, I_d)$ ,  $w_{\tau} \sim \mathcal{N}(0, I_d)$ . We  
 1136 see that for a fixed value of  $k$ , larger  $n$  yields a lower test error, which confirms our theoretical results.  
 1137

1138 Fig. 4c shows the test loss during training when training distribution is skewed and some directions  
 1139 of the downstream task are not represented enough in the training data. from  $\mathcal{N}(0, \Lambda)$  where  $\Lambda$   
 1140 is a skewed covariance matrix with eigenbasis chosen uniformly at random and  $i$ th eigenvalue  
 1141 proportional to  $1/i$ . For test, we sample prompt inputs from  $\mathcal{N}(0, I_d)$ . We use  $n = 20$ . We see that  
 1142 larger  $k$  yields a higher test error. Thus, larger test-time compute hurts the performance when some  
 1143 directions of the downstream data are not enough presented during training.  
 1144

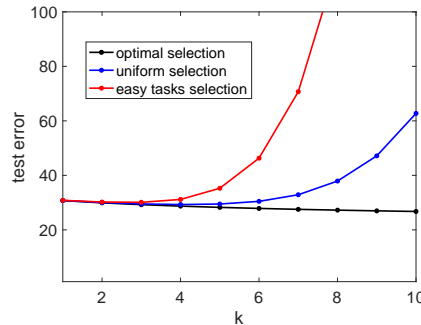


1145 Figure 4: Transformer with a single linear self-attention. (a), (b) Fixing the test error, by increasing  $k$ ,  
 1146 we can decrease the length of prompts  $n$  during training. (c) When some directions of test are not  
 1147 enough represented in training data, more test-time compute hurts the performance.  
 1148

## 1149 B.1 EFFECT OF TASK SELECTION ON TEST TIME SCALING

1150 To demonstrate the improvement we get from our task selection procedure, we consider the set up  
 1151 of Section 5.1, where we generate  $w_{\text{test}}$  with i.i.d entries from  $\mathcal{N}(0, 1)$ . During the test time we  
 1152 initialize with  $w_0 = 0$  and let the model generate the final estimate of  $w_{\text{test}}$  after  $k$  step generation.  
 1153 We set the prompt length during training to  $n = 50$  and prompt length during the test to  $m = 500$ .  
 1154 In the plot below we show how the error  $\|w_{\text{test}} - w_k\|$  behave for the following task selection  
 1155 procedures: 1) Optimal task selection: We set the probabilities  $\pi_{\ell}$  by solving the optimization  
 1156 problem (4.5). 2) Uniform selection: Where we select tasks during training with equal probability.  
 1157 3) Easy task selection: Where we select only the easy tasks (Easy-Short or Easy-Long as described  
 1158 in Section 5.1) with equal probabilities. In Figure 5, the estimation error for different task selection  
 1159 procedure is plotted versus  $k$ , the length of generations during test time before outputting the final  
 1160 estimate.

1161 As we see under the optimal choice the error goes down with  $k$ , while under the two other  
 1162 procedures the error goes up with  $k$ , indicating that a proper choice of tasks during training can avoid  
 1163 overthinking, which can occur under other choices of tasks during training.  
 1164



1165 Figure 5: Effect of task selection during training on test-time scaling  
 1166

1188 B.2 EVALUATION ON REAL REASONING BENCHMARKS  
1189

1190 We conducted new experiments to train Qwen 2.5-7B-Instruct on the OMEGA dataset (Sun et al.,  
1191 2025). We chose two tasks from the OMEGA dataset, namely GCD and polynomial root reasoning.  
1192 These tasks are designed such that training on one does not benefit the performance on the other. We  
1193 fine-tuned the base model (Qwen-Base) with RL separately on the training data of GCD and Poly.  
1194 We call these models Qwen-GCD and Qwen-Poly. We evaluate both models on the test data of GCD.  
1195 As expected, for the harder tasks that require longer reasoning, all models have a lower performance.  
1196 However, we see that while shorter test-time thinking (CoT length less than 1k characters) yields a  
1197 much better performance (+44.69%) on GCD for Qwen-GCD compared to Qwen-Base, it yields a  
1198 slightly lower performance on GCD for Qwen-Poly, compared to Qwen-Base (-1.39%). Interestingly,  
1199 when models reason for longer at test-time (between 1k and 2k characters), Qwen-Poly has a much  
1200 lower performance (-6.37%) compared to Qwen-Base, while Qwen-GCD outperforms Qwen-Base  
1201 by 11.2%. This confirms our theoretical results that when training and test data are aligned, more  
1202 thinking helps. But, insufficient task coverage in training data makes longer test-time compute  
1203 harmful.

1204 Table 1: Average accuracy on GCD for Qwen2.5-7B Instruct (Base), Base model fine-tuned on CGD  
1205 (Qwen-GCD) and Base model fine-tuned on Poly (Qwen-Poly). For all the models, the accuracy on  
1206 examples that require longer CoT is lower (compare the second column to the first column). This  
1207 confirms that examples that require longer CoT are generally more difficult. The % in () shows  
1208 the fraction of test data with the corresponding test-time CoT length. Notably, shorter CoTs (0-1k)  
1209 considerably improves the performance of Qwen-GCD (75% versus 30.39%) and slightly harms  
1210 the performance of Qwen-Poly (29% versus 30.39%). Longer CoTs improve the performance of  
1211 Qwen-GCD (38.4% versus 27.2%) and significantly harm the performance of Qwen-Poly (20.83%  
1212 versus 27.2%).

CoT length	[0, 1k)	[1k, 2k]
Qwen-Base	30.39% (30% data)	27.2% (70% data)
Qwen-GCD	75% (15% data)	38.4% (85% data)
Qwen-Poly	29% (32% data)	20.83% (68% data)

1213  
1214  
1215  
1216  
1217  
1218  
1219  
1220  
1221  
1222  
1223  
1224  
1225  
1226  
1227  
1228  
1229  
1230  
1231  
1232  
1233  
1234  
1235  
1236  
1237  
1238  
1239  
1240  
1241